Coordination Chemistry Reviews, 68 (1985) 1–52
Elsevier Science Publishers B.V., Amsterdam – Printed in The Netherlands

QUANTUM MECHANICAL EFFECTS IN INORGANIC AND BIOINORGANIC ELECTRON TRANSFER

TOM GUARR and GEORGE McLENDON

Department of Chemistry, University of Rochester, Rochester, New York 14627 (U.S.A.)

(Received 24 April 1984)

CONTENTS

A. INTRODUCTION

Electron transfer (ET) reactions have long been a central focus of mechanistic inorganic chemistry [1–12]. This interest stems partly from the fact that many transition metal complexes are versatile redox reagents. The wide range of oxidation states available over a comparatively narrow energy range often makes electron transfer reactions both thermodynamically and kinetically facile.

Inorganic redox reactions are also of primary importance in biological systems. Indeed, some of the most elegant work and intriguing data come from the area of inorganic biochemistry [11,13–17].

Likewise, a great deal of research has been devoted to excited state chemistry, taking advantage of the increased electron affinity and lability of

0010-8545/85/$18.20

these systems. Work in this area covers everything from solar energy storage schemes [18–27] to studies on natural photosynthetic centers [28–32].

Over the last two decades, a guiding principle for work on electron transfer has been the classical (in every sense) theory of electron transfer as developed by Marcus [1–4], Hush [5,6] and others [33,34]. A number of excellent reviews and monographs of this work are available [4,8–12].

However, within the past few years, increased theoretical and experimental attention has focused on nonclassical (i.e. semiclassical and quantum mechanical) aspects of electron transfer reactions, e.g. electron (and nuclear) tunneling reactions [35–55]. These quantum mechanical phenomena are critical for understanding many details of inorganic electron transfer, including virtually all bioinorganic electron transfer reactions.

Thus this review has three aims. First, it (hopefully) provides a physically meaningful sketch of the current state of quantum theories of electron transfer, and briefly compares the quantum and classical (Marcus) theories.

Second, some experimental data on quantum effects in electron transfer are presented. In truth, relatively few clear examples of quantum effects are available. This is not because such effects are rare. However, until recently, few experiments were designed to focus on such effects. Fortunately this situation is rapidly changing. Therefore it is not the intent of this paper to produce an exhaustive review of the meager data available, since any such "catalog" would be outdated immediately. Instead, a few illustrative examples of quantum manifestations in electron and nuclear tunneling reactions are provided.

Finally, as the foregoing comments indicate, this area of investigation is young and rapidly developing. A final goal of the review is to help highlight the many areas where further work could provide significant advances.

B. CLASSICAL THEORY

Each of the classical theories proposed in the literature begins with its own unique set of assumptions and approach to the problem. One assumption common in all purely classical theories is that all ET reactions are adiabatic. In other words, the reaction occurs on a continuous path on a single potential surface. A simplified, two-dimensional picture is shown in Fig. 1. In this Figure, the reactant and product potential curves (representations of multi-dimensional potential surfaces) are drawn along a reaction coordinate q. The positions of all the nuclei in the system (including solvent and both reactants) are represented by the value of q. Hence, the horizontal displacement of the two wells gives an indication of the extent of nuclear motion involved (the strength of coupling) in the electron transfer event.

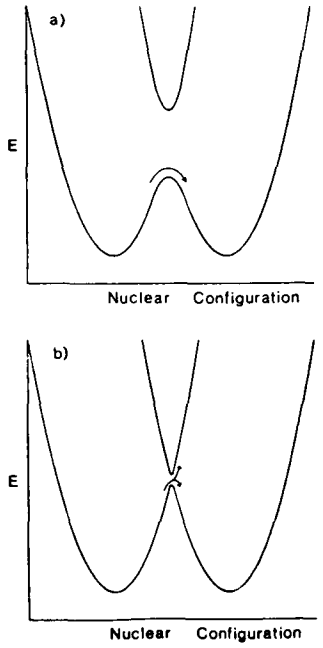

Fig. 1. (a) Potential surface for an adiabatic electron transfer reaction. (b) Potential surface for a nonadiabatic electron transfer reaction. Arrows in both (a) and (b) indicate possible pathways available to the system on moving from reactants (left well) toward products (right well).

The energy involved in moving all the nuclei to their appropriate positions is referred to by Marcus [1–4] as the reorganization energy, λ, from inner sphere effects (λ_{in}) and from outer sphere effects (λ_{out}). λ_{in} includes changes in bond angles and bond lengths in the reactant and product molecules themselves. λ_{out} includes changes in solvent configuration, and is largely due to the repolarization energy of the solvent. λ_{out} can be defined as

$$\lambda_{out} = \frac{(\Delta e)^2}{4\pi\epsilon_0}\left(\frac{1}{2a_1} + \frac{1}{2a_2} - \frac{1}{r_{12}}\right)\left(\frac{1}{D_{op}} - \frac{1}{D_s}\right) \tag{1}$$

where Δe is the charge transferred, ϵ_0 is the permittivity of free space, a_1 and a_2 are the radii of the reactants, $r_{12} = a_1 + a_2$, and D_{op} and D_s are the optical and static dielectric constants of the medium, respectively.

As an example, λ_{out} can be calculated for the $Fe(H_2O)_6^{2+/3+}$ self-exchange reaction in water as follows. The following values are used in eqn. (1). $a_1 = 3.43 \times 10^{-10}$ m, $a_2 = 3.57 \times 10^{-10}$ m, $r_{12} = 7 \times 10^{-10}$ m, $D_{op} = n_0^2 = 1.78$, and $D_s = 78.5$. In addition, $\Delta e = 1.6 \times 10^{-19}$ C and $\epsilon_0 = 8.85 \times 10^{-12}$ Fm^{-1}. Substitution yields

$\lambda_{out} = 1.8 \times 10^{-19}$J = 109 kJ mol^{-1} ($\sim$ 1.1 V)

However, we note that a dielectric continuum model may not be appropriate for the case of a highly-structured solvent like water. Furthermore, recent work suggests that solvent reorientation may become "rate limiting" in some cases. In such instances T.S. models are invalid [203,226,227] and are replaced by an expression like $k = \nu \exp - \Delta G^*/kT$ where $\nu \times 1/\tau_{\text{longitudinal}} = (\epsilon_\infty/\epsilon_s)\tau_0$ where τ_0 is the Debye relation time.

Calculation of λ_{in} is more complex. λ_{in} can be defined as

$$\lambda_{in} = (1/2)\Sigma F_j \Delta Q_j^2 \tag{2}$$

where F_j represents Hooke's law force constants, approximated by averaging the appropriate force constants of reactant and product

$$F_j = \frac{2F_{\text{reac}}F_{\text{prod}}}{(F_{\text{reac}} + F_{\text{prod}})} \tag{3}$$

and ΔQ_j represents the displacement of the equilibrium position in the jth normal mode.

Siders and Marcus [56] have pointed out the necessity of including cross-terms in this calculation, since off-diagonal force constants are obtained when the symmetric stretching mode (the reaction coordinate) is expressed in terms of bond modes. A series of elegant experiments relating λ_{in} (and thus rate) to specific bond dislocations have been reported by Sutin [222] and coworkers as an example.

Values of λ_{in} vary widely, from 0 (no change in bond lengths) to > 1 V. For example, λ_{in} for the $Fe(H_2O)_6^{2+/3+}$ self-exchange can be calculated to be ~ 140 kJ mol^{-1} (~ 1.4 eV) [56]. This large value is a direct consequence of the 0.14 Å bond length difference between the oxidized and reduced states.

Thus, the horizontal displacement between the two curves in Fig. 1 accounts for changes in both solvent (λ_{out}) and reactant (λ_{in}) nuclear coordinates. Electron transfer occurs when the system attains a geometry intermediate between that of reactants and products, corresponding to the intersection of the potential surfaces.

At the intersection of the two curves, there is an "avoided crossing" caused by the overlap of the reactants' electronic wavefunctions. This overlap causes a splitting of the two surfaces by an amount $2H_{ab}$. The magnitude of this "interaction energy" depends on the distance between and orientation of reacting partners and the degree of shielding of the electronic orbitals. A totally adiabatic reaction occurs when H_{ab} is large enough ($H_{ab} > \sim 100$ cm^{-1}) for the system to remain on the lower surface when proceeding from reactants to products. According to Marcus [1–4], the rate of collisional process in solution can be expressed as

$$R = kT/h(\kappa \exp(-E_{act}/kT)) \tag{4}$$

where k is Boltzmann's constant and κ represents the probability of a system in the transition state being converted to products. For an adiabatic reaction, $\kappa = 1$.

Neglecting work terms

$$E_{act} = (\Delta E - E_r)^2/4E_r \tag{5}$$

where $E_r = (\lambda_{in} + \lambda_{out})$, the total reorganization energy.

For a self-exchange reaction, $\Delta E = 0$ and, from eqn. (5), $E_{act} = E_r/4 = (\lambda_{in} + \lambda_{out})/4$. Thus, for example, E_{act} for the $Fe(H_2O)_6^{2+/3+}$ exchange is calculated to be (1.4 V + 2.2 V)/4 ≅ 0.63 V. As mentioned, this calculation does not include the work required to bring the reactants together (work terms). Note that, for a given reorganization energy E_r, eqn. (5) yields decreasing values of E_{act} with increasing reaction exothermicity.

Generally, in a diffusional reaction, the electronic interaction, and hence the splitting between surfaces, is thought to be large (a few hundred cm^{-1}). However, when H_{ab} is small ($H_{ab} \lesssim 10\ cm^{-1}$), the splitting between surfaces is small, and the system can sometimes "jump" to the upper surface. It may therefore pass through the transition state many times without proceeding on to products. Such a system is said to be "nonadiabatic" and κ is less than unity.

A small interaction energy can arise from unfavorable orbital symmetries, changes in spin multiplicity, or large donor–acceptor separation distances. For biochemical systems or reactions of molecules in rigid matrices, large separation distances are involved, and a nonadiabatic model is needed to interpret such reactions.

Another way in which nonadiabaticity is introduced in a reaction is through nuclear tunneling. In Fig. 1, the top of the barrier represents the formation of a "precursor complex", which has a geometry intermediate between that of reactants and products. In any given reaction, there is a small, yet finite, probability that the system will tunnel through the barrier rather than surmount it. This pathway becomes more significant, of course, when the barrier is very high (reactants and products have very different geometries) or the temperature very low.

It may be useful to point out the difference between electron and nuclear tunneling, as they have often been confused in the literature. Both are quantum mechanical phenomena which involve a particle tunneling through a barrier. However, the barrier is not the same for electron and nuclear tunneling. Figure 1 shows potential surfaces plotted versus nuclear coordinates. Thus, any tunneling through this barrier involves nuclear motion, and hence is nuclear tunneling.

Electron tunneling always occurs at the instant of transfer. At that instant, the nuclei are fixed at the (intermediate) geometry which allows conservation

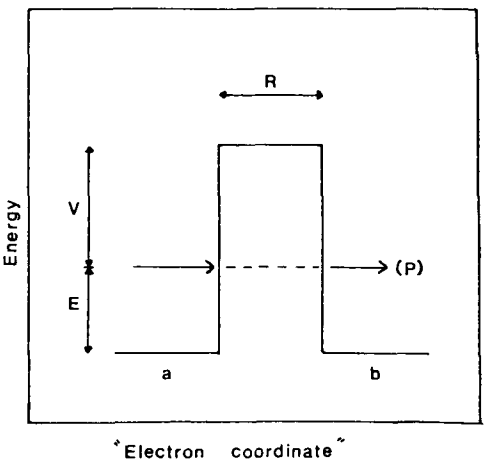

Fig. 2. One-dimensional barrier model for quantum mechanical tunneling processes. The probability, (P), of passage through the barrier is related to the barrier height (V) and width (R). The abscissa is a fictionalized "electron coordinate".

of energy during electron transfer. Thus the diagram in Fig. 1 is not helpful. The term "tunneling" when applied to the electronic frequency factor derives from consideration of transmission through a classically impenetrable barrier, as shown in Fig. 2. Such a barrier is conveniently thought of as a "space" between reactants where an electron is a high energy species. This "space" can be filled by intervening solvent molecules, protein, membrane ,... etc. The height of this barrier, V, is simply the difference in vertical (without allowing for nuclear relaxation) affinities between the oxidized donor and the intervening barrier.

The probability of tunneling so calculated depends exponentially on the barrier width and is given by the Gamow tunneling equation [57].

Probability of barrier penetration $= 16\, EV/(E+V)^2$

$$\exp\left(\left(-2b(2mV)^{1/2}\right)/h\right) = C\exp(-2\alpha b) = C\,|H_{ab}|^2 \tag{6}$$

where E = kinetic energy of the electron, m = electron mass, b = barrier width, and V = barrier height and α = damping factor accounting for the fall off of wavefunction overlap with distance.

In many situations (for example, most collisional redox processes) the barrier width will be negligibly thin and "tunneling" will have no effect on the rate of net electron transfer. Thus, the reaction is adiabatic. The appearance of $|H_{ab}|^2$ in a rate expression does not necessarily imply a nonadiabatic mechanism. It suggests only that the rate of the reaction is sensitive to changes in the electronic coupling between reactants. Histori-

cally, electron "tunneling" has been used as a descriptive term to imply a weak electronic coupling which leads to nonadiabatic ($\kappa < 1$) transfer. For example, if the reactants are separated in space with a nonconducting medium between them, the barrier is significant. However, in a collisional process, the barrier may be very thin, resulting in a large interaction energy and tunneling is facile. The two surfaces are sufficiently separated so that the reaction becomes adiabatic and "tunneling" as such does not affect the rate of product formation. In other words, for an adiabatic reaction ($\kappa = 1$) changes in the electronic coordinates are instantaneous on the vibrational timescale, and the frequency term reduces to an (averaged) vibrational frequency of approximately 10^{13} s^{-1}. Such a tunneling description has been tested in solid-state physics, where it has proven quite successful. For molecular systems, other ways of predicting the dependence of electron transfer rates on donor–acceptor distance can surely be imagined.

A chemically-appealing model, based on the principle of superexchange, has been suggested by McConnell [121] and elaborated by several authors [81,122]. A particularly readable account is offered by Beitz and Miller [81]. In essence, these authors postulate a mechanism whereby long range electronic coupling is propagated via a series of nearest neighbor superexchange interactions involving orbitals of appropriate energy. For such an interaction the total interaction potential will depend on the exchange integral, β, the number of exchanges, n, and the ionization potential B of the donor. Thus $V_{el} = B(B/\beta)^n$ (note that in this model coupling may occur via LUMO's (e^- states) or HOMO ("hole transfer" states). Since the number of exchanges scales with donor acceptor distance, R, (i.e. $n = R/d$, where d is the (average) nearest neighbor separation). We thus obtain $V_{el} = \exp - \alpha R$ where $\alpha \approxeq 1.1$. Thus, both models predict an exponential dependence of rate on distance. However an important difference exists between the barrier tunneling model and the superexchange model. For barrier tunneling α = constant $\times$ (binding energy)$^{1/2}$, whereas for superexchange α = constant $\times$ ln(binding energy). In essence, in the superexchange model, the long distance electron transfer depends only weakly on the precise donor bonding energy, or on the orbital energies of the medium, while barrier tunneling is quite sensitive to both their parameters.

An interesting application of superexchange type coupling in inorganic redox reactions has been suggested by Endicott et al. [224]. These workers found that specific halides and pseudo halides could greatly accelerate electron transfer apparently by a mediated increase in donor–acceptor coupling strength.

One specific case which is related to this general superexchange model should be briefly mentioned. Hush has suggested a mechanism for long-range through bond coupling which rate depends only weakly on distance, rather

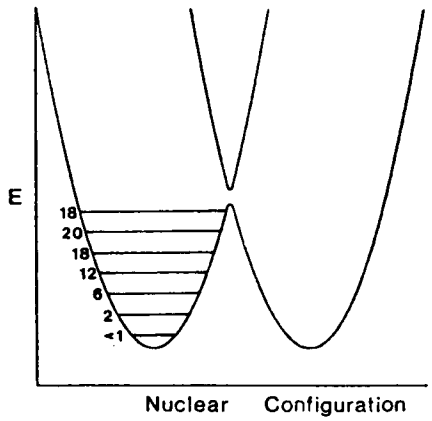

Fig. 3. Percent contribution to the rate of the $Fe(H_2O)_6^{2+/3+}$ self-exchange at 300 K from reactants in a given vibrational level. Calculated using a one-dimensional model with $E_r = 25.6$ kcal mol^{-1}. Numbers to the left of each reactant vibrational level represent their percent contribution to the total reaction. This figure is adapted from ref. 47.

than exponentially. As yet insufficient data are available to test these predictions. However, Beratan and Hopfield [122] have used an explicit molecular orbital treatment of through bond electron transfer for the homologous $Ru^{II}S\ (C_n) - \delta - Ru^{III}$ compounds studied by Stein et al. [118]. These theoretical results closely reproduce the experimental data, and suggest that the redox reaction is mediated by hole exchange (analogous to valence band conduction) rather than electron exchange via a conduction band.

Like electron tunneling, nuclear tunneling can have several important implications for the behavior of electron transfer systems. Recall that in eqns. (2) and (3), λ_{in} involved nuclear motion along an intramolecular mode of frequency $h\omega$ (typically several hundred wavenumbers). If $h\omega \ll kT$, then a classical (Boltzmann) population distribution can be assumed and Arrhenius behavior is expected as in eqn. (4). However, when $h\omega \geqq kT$, some portion of the total reaction will proceed via nuclear tunneling [47] (see Fig. 3). In the limit where $h\omega \gg kT$, all of the reaction must proceed by nuclear tunneling [58]. A slow, temperature-independent rate will be observed [59]. Thus, experimental evidence of quantum effects in ET reactions might be gathered from studies of rate as a function of temperature.

Such effects might also be manifested on isotopic substitution of the reactant complexes for which the intramolecular reorganization, λ_{in}, is significant. This kinetic isotope effect (KIE) arises from the fact that isotopic substitution causes a change in the associated vibrational frequency, which leads to a change in the width (and height) of the nuclear barrier to electron transfer (Fig. 3).

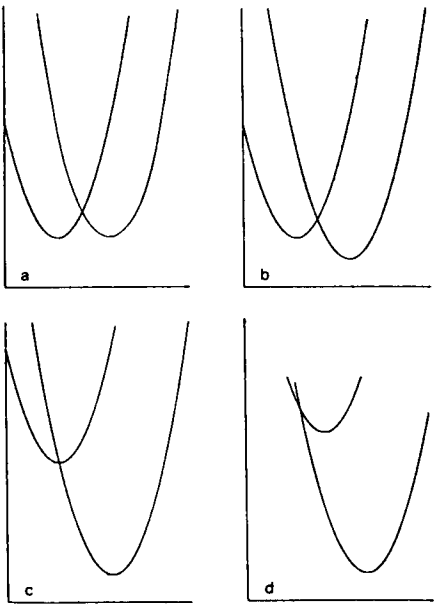

Fig. 4. Potential surfaces for electron transfer reactions as a function of driving force. ΔE increases from (a) to (d).

A further distinction between classical and quantum theories of ET concerns the dependence of rate on the separation distance between reactants. As long as the reaction is adiabatic, then the rate will decrease slowly as R increases, reflecting the dependence of λ_{out} on R. In adiabatic theories, the electronic interaction between reactants is presumed to be strong. (Here "strong" means merely a surface splitting in Fig. 1 > ca. 100 cm^{-1}!) For an adiabatic reaction, the rate depends only on the probability of reaching the transition state through appropriate nuclear fluctuations. However, by definition for nonadiabatic transfer, the reaction does not occur every time a favorable nuclear geometry is attained. Rather, the probability of product formation from the classical turning point is related to the magnitude of the electronic interaction, H_{ab}, which is in turn a function of distance.

Particularly important detailed calculations have been carried out by M. Newton for the Fe^{2+}/Fe^{3+} (aq.) couple. It appears that electron transfer is (weakly) nonadiabatic for this couple, even at VDW contact distances.

Finally, differences between classical and quantum rate predictions are expected at high driving forces. Figure 4 shows a very simplified picture of the classical dependence of rate on ΔE. Figure 4(a) depicts a self-exchange reaction, where $\Delta E = 0$. In Fig. 4(b), a slightly more exothermic reaction is shown, with a resulting lower activation barrier. In the limit of $\Delta E = E_r$

(Fig. 4(c)), the product potential curve passes through the minimum on the reactant curve, $E_{act} \equiv 0$, and the rate is maximized. If the reaction becomes even more exothermic (Fig. 4(d)), the intersection is now to the left of the reactant minimum, and the activation barrier grows. This leads to a decrease in rate with increasing exothermicity and is one of the most interesting predictions of Marcus theory. Marcus predicts a quadratic dependence of rate on ΔE in this so-called "inverted region" (eqns. (4) and (5)). As we can see, in Fig. 4(e), quantum mechanical descriptions modify, but do not abolish this prediction.

In summary then, there are at least four areas which can yield information on quantum effects in electron transfer reactions: (a) temperature dependence of rate (especially at low temperature); (b) manifestation of kinetic isotope effects; (c) dependence of rate on donor-acceptor distance; (d) differences between classical and quantum rate predictions when $\Delta E > E_r$.

Before discussing the experimental work in these areas, we shall briefly review the evolution of quantum theories.

C. DEVELOPMENT OF THEORY

All useful nonadiabatic theories contain two important components, an electronic factor and a nuclear factor. The nuclear, or Franck–Condon term, contains essentially all of the dependence on ΔE, λ, and temperature. In fact, studies of the temperature dependence of electron transfer supplied the initial impetus to develop theoretical expressions containing appropriate nuclear terms. The electronic term describes the extent of electronic coupling and hence the dependence of rate on distance. The form of the electronic factor is commonly given by the Gamow tunneling equation [57] although, as we shall see, a superexchange model may be more appropriate (see Fig. 2 and eqn. (6)). Since many of the expressions were originally derived to describe biological systems, it will be useful to note briefly the special aspects of biological electron transfer.

The biological problem differs from the problem of electron transfer between simple ions in solution in several ways. First, the effects of reactant diffusion are absent. The biological molecules form reactant pairs, and thus we are concerned only with electron transfer within this "supermolecule". Secondly, the active sites in this "supermolecule" are separated by a single, fixed distance ranging from several Ångstrom units to ca. 25 Å. Thus we can expect the reaction to be nonadiabatic. Last, proteins are often considered limiting cases of a low dielectric media. As such, the medium reorganization energy may be low (unlike solution processes) and higher frequency intramolecular modes may dominate the reorganization term. This, in turn, could lead to quantum effects.

D. THE SEMICLASSICAL APPROXIMATION

Hopfield, using an analogy to the Förster–Dexter theory of energy transfer, developed a semiclassical theory of electron transfer [39]. Hopfield used this theory to fit the temperature dependence of the rate of cytochrome c oxidation in *C. vinosum*, as reported by DeVault and Chance [13].

Hopfield's rate expression is

$$W = (2\pi/h)\,|H_{ab}|^2 (1/2\pi\sigma^2)^{1/2} \exp(-E_a - E_b - \Delta)^2/2\sigma^2) \tag{7}$$

where

$$\sigma^2 = (k_a x_a^2/2)\kappa T_a \coth T_a/2T + (k_b x_b^2/2)\kappa T_b \coth T_b/2T \tag{8}$$

$\Delta = \frac{1}{2}k_a x_a^2 + \frac{1}{2}k_b x_b^2$, k = Boltzmann's constant, k_a and k_b are Hooke's law force constants for vibrations of species a and b, and x_a and x_b represent displacement of nuclear coordinates from their equilibrium positions.

With appropriate choice of parameters, this expression seems to fit the data quite well [39]. The temperature dependence (at high T) of Hopfield's expression can be traced to temperature dependences in his "electron removal" and "electron insertion" spectra.

It has been suggested that electron transfer is not analogous to energy transfer [40,60]. Förster–Dexter theory [61,62] assumes coupling of the donor and acceptor to different sets of oscillators, while the larger perturbation of an electron transfer event would likely cause both to couple to similar phonon fields in the medium. Only in the limit of no medium reorganization (intramolecular modes dominate) would the donor and acceptor be coupled to a different oscillator field.

E. PURELY QUANTUM FORMULATION

In 1976, Jortner formulated the problem of biological ET in terms of a nonadiabatic multiphonon nonradiative decay process. Jortner's model [40] rests on the analogy between electron transfer in a well-defined reactant pair and an ordinary unimolecular radiationless decay [63]. A single mean frequency $\langle\omega\rangle$ is used to characterize the intramolecular reorganizational modes. Similarly, the low-frequency medium reorganizational modes are characterized by $\langle\omega_s\rangle$, the mean frequency of the solvent modes.

It is important to note that, for this kind of analysis, there are three distinct regions in a rate vs. temperature plot.

(1) Extremely low temperature region. In this region $kT < h\langle\omega_s\rangle \ll h\langle\omega\rangle$. No modes can be thermally populated, and the reaction must occur by

nuclear tunneling. It occurs from the zero point of the reactant well to any accessible state (must be nearly degenerate) on the product surface. The rate is temperature independent.

(2) Intermediate (transition) region. In this region $h\langle\omega_s\rangle < kT \ll h\langle\omega\rangle$. This corresponds to the case in which thermal energy enables the system to move part of the way up the well, and nuclear tunneling occurs from this higher level. The reorganization of the low-frequency mode occurs classically, while the system must still tunnel through the barrier corresponding to reorganization of a high-frequency (intramolecular) mode. The rate here is temperature dependent, with an apparent activation energy due to the classical rearrangement (low-frequency mode) only.

(3) High temperature region. In this region, $h\langle\omega_s\rangle \ll h\langle\omega\rangle < kT$. The system behaves classically. The rate is temperature dependent, with the activation energy being given by the Marcus expression (eqn. (5) with E_r = total reorganization energy).

Jortner analyzed the data of DeVault and Chance [13] on *C. vinosum* according to this model. Since the transition temperature was too high to allow for strong coupling to the medium modes, he asserted that the coupling to low frequency phonon modes was negligible while coupling to intramolecular modes was extremely strong. The data fitted well with $\Delta E = 0.1$ V, $h\langle\omega\rangle = 400\ \text{cm}^{-1}$, $S = 20$, and A (a pre-exponential factor = $2\pi|H_{AB}|^2/h^2\omega) = 10^9$.

The theory, as presented by Jortner, is fully quantum mechanical and reduces to classical Marcus theory in the high temperature limit. We quote only the final (general) result here

$$W_{ab} = 2\pi\left(|H_{ab}|^2/h^2\omega\right)\exp[-S(2\bar{\nu}+1)] \times I_p\left\{2S\left[\bar{\nu}(\bar{\nu}+1)\right]^{1/2}\right\}\left[(\bar{\nu}+1/\bar{\nu})^{p/2}\right] \tag{9}$$

where $I_p\{\}$ is the modified Bessel function of order p, $p = \Delta E/h\omega$ is the energy gap in units of vibrational quanta, $S = E_{in}/h\omega$ is the inner-sphere reorganization energy in units of vibrational quanta (E_{out} is assumed equal to zero here), and $\bar{\nu} = [\exp(h\omega/kT) - 1]^{-1}$.

Kuznetsov, Søndergård, and Ulstrup have allowed for a spread of frequencies involved in coupling to the medium [43]. Utilizing a frequency distribution of the Debye form, they were able to fit the low temperature branch of the *C. vinosum* data [13] with a medium reorganization energy of 0.2–0.4 eV. They argue that: (1) the cytochrome c may be localized in an aqueous phase; (2) membrane packing may need to reorganize following electron transfer; (3) activationless behavior at low temperatures is related to

the fact that the number of thermally accessible modes is proportional to the temperature at very low temperatures.

These workers also note that frequencies associated with polarization and conformational changes are too low to contribute significantly to the reorganization energy (in light of the temperature-independence up to ~ 100 K. Rather, they contend, modes involving hindered translation and rotation (50 to several hundred cm^{-1}) are important [43].

The inclusion of an intramolecular mode with $h\omega \cong 400$ cm^{-1} was necessary to reproduce the high-temperature branch of the data, although the coupling constant ($S = 8$–9) was somewhat lower than that found by Jortner [40] ($S \cong 20$). This, of course, is due to the hypothesis of stronger coupling to medium modes (in addition to the different value of ΔE used).

Dogonadze et al. [38] report results using not only a Debye distribution, but also a general expression. In the limit of a sufficiently narrow distribution, the expression reduces to the transition probability for a system considering only a single mode, as first developed by Lax [64].

Buhks et al. have suggested that the Debye model is inappropriate for electron transfer processes [50]. These workers utilize a distribution which roughly describes the optical normal modes of ice. The mean frequency value used $h\omega_0$, was 200 cm^{-1}, and the width of the distribution, $h\Delta\omega = 200$ cm^{-1}. Using a single mode approximation for the high frequency modes, with $h\omega_c = 500$ cm^{-1}, they obtain a reasonable fit to the DeVault and Chance data [13]. However, the value used for the intramolecular reorganization energy, $E_c = 17500$ cm^{-1} (~ 2.2 eV) seems quite large. Further, the value for the electronic coupling matrix element, $V \sim 90$ cm^{-1}, which was obtained is much larger than expected. Indeed, if this value is correct, it would cast doubt on a basic premise of the model, that of the assumption of nonadiabiatic behavior.

Recently, Sarai [53,54] has considered the effect of coupling to a number of discrete low-frequency protein modes rather than a continuum of medium modes. Unfortunately, this work is rather qualitative.

Kakitani and Kakitani have developed a treatment which accounts not only for changes in equilibrium bond lengths, but also for frequency shifts during electron transfer [52]. Their results are similar to those of Jortner [40], except that ΔE, the energy gap, is replaced by $-\Delta G$, the free energy gap.

In fact, the final expression quoted by Kakitani and Kakitani is identical to that of Jortner (eqn. (9)), except that p is now defined as

$$p = \left(\Delta E + \sum_j \left(h\Delta\omega_j/2 \right) + \sum_j \bar{n}_j j h\Delta\omega_j \right) \tag{10}$$

with $\bar{n}_j = (\exp(h\omega_j/kT) - 1)^{-1}$

The last two terms in the expression for p account for differences in zero point energies and free energy, respectively, due to frequency shifts in the jth mode of the system [52]. Thus, in large part, the temperature dependence of ΔG accounts for the overall temperature dependence of the rate. They are able to fit the data of DeVault and Chance [13] using an extremely small coupling constant, $S = 0.5$. As expected, a major contribution to the temperature dependence comes from the variation of ΔG with temperature. ΔG varies from -0.45 V [65] at 300 K to -0.88 V at 4 K. These workers use an average frequency $\langle v \rangle = 1000\ \text{cm}^{-1}$ for the reorganized intramolecular modes and discount the solvent modes entirely. The high value of $\langle v \rangle$, they contend, is supported by resonance Raman work [66] if the contribution of solvent modes is negligible.

Kakitani and Kakitani are also able to fit the negative activation behavior of the back electron transfer in the *Rps. sphaeroides* photosynthetic system [31] with appropriate choice of parameters [52]. Further, they are able to explain the huge difference in the forward and reverse reaction rates in the photoexcited bacteriopheophytin [67] system. This is possible since, in their model, $S \ll p$ and thus most biological electron transfers with moderate $-\Delta G_{\text{rxn}}$ are in the so-called "inverted" region. With $S = 0.5$–1.0, the falloff of rate with $-\Delta G_{\text{rxn}}$ (Δp) is quite steep [52].

F. COMPARISON OF THEORETICAL TREATMENTS

Given the discrepancies between the various treatments even when evaluating identical data sets, one might well ask which theories, if any, are more nearly "correct". The values of the "best-fit" parameters to the *C. vinosum* data using the most popular treatments are summarized in Table 1.

Column 1 lists the different values assumed for ΔE, the reaction driving forces. The fact that it is not a known quantity illustrates one of the many problems associated with biological transfers. However, a reasonable guess for the value of ΔE is the difference in midpoint potentials of the species involved, ~ 0.45 V [16,38,65]. While this alone does not discredit the Hopfield [39] and Jortner [40] treatments, it certainly casts doubts on the validity of the other fitted parameters.

Blankenship and Parson have applied Jortner's theory to the problem using the more "correct" value of $\Delta E = 0.45$ V [16]. They find that extremely large coupling constants are necessary to fit the data. This leads to physically unrealistic values for the inner-sphere reorganization energy of more than 2 V. Assuming the $\sim 400\ \text{cm}^{-1}$ metal–ligand stretch is the primary accepting mode, this would correspond to displacement of the iron by roughly 0.4 Å [52]. Further, as pointed out by the authors, the calculated value of H_{ab} is

TABLE 1

Comparison of the theoretical treatments of electron transfer with regard to the data of DeVault and Chance

Treatment	ΔE (V)	$\hbar\omega_{in}$ (cm^{-1})	S_c	E_c (V)	$\hbar\omega_{out}$ (cm^{-1})	S_s	E_s (V)	H_{ab} (cm^{-1})	Ref.
Hopfield	0.05	250	33	1.0	–	0	0	3	39
Jortner	0.1	400	20	1.0	–	0	0	0.1–0.4	40
Blankenship and Parson	0.45	400–500	44–48	2.2–3.0	40	~0	0	8–80	16
Kuznetsov et al. (c.f. Dogonadze et al.)	0.45	400	8–9	0.4	~150 (Debye dispersion)	~13	0.25	1–10	43
Buhks et al.	0.45	500	37	2.3	0–400 (dispersions)	~10	0.12–0.37	90	50
Kakitani and Kakitani	0.45 (~300 K) to 0.88 (4 K)	1000	0.5	0.06	–	0	0	0.5	52

quite large and may even contradict the assumption of nonadiabatic behavior. Similar arguments apply to the treatment of Buhks et al. [50].

Kuznetsov, Søndergård, and Ulstrup [43], in accord with a more general expression advanced by Dogonadze et al. [38], are able to fit the data using reasonable values of the various parameters. However, the appropriateness of the Debye distribution in this particular case has been questioned [50]. It remains uncertain whether this description corresponds to physical reality.

Finally, Kakitani and Kakitani have included the effects of frequency shifts, and employed the notion of very weak coupling to a high average frequency [52]. While the idea that essentially all biological electron transfers are inverted cannot be rejected a priori, the few data available do not support this notion. Additional work involving systems with different ΔE values would be useful in this regard.

From the foregoing discussion, it is apparent that many different approaches to the problem can be taken. With this in mind, the available data concerning the quantum nature of the ET process will be examined.

G. DISTANCE DEPENDENCE

We first turn our attention to the final column in Table 1. Interestingly, the calculated H_{ab} values vary by nearly 3 orders of magnitude. Since this term contains essentially all the distance information of the system, it is obvious that at present there is no widespread agreement on the distance scale for electron transfer. Estimates range from a few Ångstroms [11] to the 100 Å distance reported by Horne for electron transfer in ice [11,68,69].

As previously described in eqn. (6) and Fig. 2, the dependence of electron transfer rate on distance arises from the Gamow factor, which is incorporated into the electronic interaction matrix element. The damped exponential form of this dependence was established 50 years ago [57], although it has been applied to simple electron transfer reactions only recently. Conflicting distance scales are often due to using different values for the barrier height, V.

Hopfield [39] postulated an expression for H_{ab} (T_{ab} in Hopfield's notation) to account explicitly for the distance dependence of rate

$$T_{ab} \cong \left(2.7/(N_a N_b)^{1/2}\right) \exp(-0.72R) \tag{11}$$

where R is edge-to-edge distance between π-systems (in Å) and N_a and N_b are the number of atoms in the π-systems involved.

To obtain this expression, Hopfield made several important assumptions: (1) The factor $(N_a N_b)^{-1/2}$ arises from the assumption that the wavefunction of the tunneling electron should be spread out over the conjugated atoms. It also allows for interaction to occur through only one atom of each π-system.

(2) The factor 2.7 was obtained by setting the electron exchange integral at 1 eV for interaction between two carbon atoms at a typical bonding distance. Unfortunately, nonadiabatic electron transfer is not entirely analogous to interaction between two carbon atoms at distances small enough for bond formation. (3) The exponential damping factor, 0.72, is a consequence of the assumption of a 2 eV barrier height.

The estimation of barrier height is particularly important here, as it appears in an exponential term. This barrier height, as shown in Fig. 2, is simply the difference in vertical electron affinities of the oxidized donor and the medium. While Hopfield uses a value of 2 V [39], Jortner [40] postulates a barrier height of ~ 6.4 eV.

A more recent discussion by Buhks and Jortner [46] suggests a barrier height of ~ 3.8 eV. In reality, of course, the barrier height depends on the electron affinity of the donor, as pointed out by Redi and Hopfield [70] and DeVault [11]. At present, it is unclear whether any one of the estimates is valid for any particular system of interest. It is, however, certain that none of the proposed barrier heights is universal.

Unfortunately, there has often been a tendency in the literature to use one of these distance scales without questioning its validity. The discrepancies which can be caused by different parameter selection are striking

Rate $\propto \lvert H_{ab} \rvert^2 \propto e^{(-1.44R)}$	Hopfield [39]
$\propto e^{(-2R)}$	Buhks and Jortner [46]
$\propto e^{(-2.6R)}$	Jortner [40]

Assumption of a 10 Å distance between donor and acceptor, as in biological systems, produces a 10^5 predicted rate differences in ref. 39 vs. ref. 40. By comparison, the superexchange model already discussed [81] makes a quite different prediction for the dependence of rate on V.

Since the binding energy only enters as one of many electronic coupling terms, $H_{AB} = \ln(V/\beta)$. The superexchange model and barrier tunneling models thus agree that H_{AB} depends exponentially on distance, but strongly disagree on the dependence of rate on electron binding energy. For barrier tunneling, a strong dependence is expected, while for a superexchange mechanism, a weak dependence of $k(R)$ on V is predicted.

H. EXPERIMENTAL DISTANCE DEPENDENCE

As previously mentioned, factors such as different orbital symmetries and spin multiplicities can also introduce nonadiabaticity. In fact, there is evidence that reactions involving the $Eu^{2+/3+}$ couple may be strongly nonadiabatic [71–73]. However, systems in which $\lvert H_{ab} \rvert$ is measured (or inferred) as a function of distance are far more prevalent and will be the focus of this

section. The study of such distance dependences in homogeneous fluid solution poses obvious problems, and most experimentalists work in systems where diffusion is absent [74].

Experiments designed to probe the distance dependence fall into two general classes: (1) methods which involve a distribution of donor–acceptor distances around some average value, R_{avg} (i.e. electron transfer between two isolated molecules in a rigid matrix); (2) methods which rely on a fixed donor–acceptor separation, as in intramolecular electron transfer, in a molecule containing both functionalities.

There are distinct advantages and disadvantages within each approach, and these will be discussed in some detail.

(i) Experiments in rigid matrices

In this class, one reactant is generally present in a great excess over the other. The assumption is usually made that the distribution of this species in the matrix is random. Since it is present in excess, its spatial distribution controls the average donor–acceptor separation. This distance can be varied in a systematic way simply by changing the concentration of the excess reactant.

Most of the work in this area has involved pulse radiolysis in an optical glass. In particular, Miller and coworkers [77–83] and others [84–86] have extensively studied reactions of trapped electrons with various acceptors in a number of glasses. In these experiments, the concentration of trapped electrons is monitored as a function of time.

Recently, reports of photoinduced electron transfer in rigid matrices have appeared [82,83,87–89]. The situation is entirely analogous to that involved in the pulse radiolysis work and the following discussion is applicable to either case. First, recall equation (6), which simply states that the rate of an ET reaction is proportional to $\exp(-2\alpha R)$. The goal of many of these studies is to obtain a reasonable value for α. A typical experiment involves transfer from a photoexcited donor to a ground state acceptor in a glass. The ET rate is measured (i.e. by fluorescence quenching or transient absorption techniques) as a function of acceptor concentration (Fig. 5).

The data are first analyzed to obtain a "critical distance" parameter [90]. Roughly speaking, this is the distance at which electron transfer becomes competitive with normal decay channels [82]. That is

$$k_{ET}(R_{crit}) \cong \frac{1}{\tau_0}$$

However, such long distances require that the Franck–Condon factors must be optimized. This follows from the fact that the "critical" rate $k(R) = 1/\tau_0$

is a product of electronic and nuclear frequency factors. When the nuclear frequency factor is optimized, the electronic factor can be reduced, while still maintaining a rapid rate. For example, for the $Ru(bpy\text{–}X)_3^{2+}$* + TMPD reaction, when ΔE is decreased from ~ 0.8 V to 0.2 V, R_{crit} decreases from 19 Å to 12 Å (i.e. maximum R). "Critical distances" for photoinduced electron transfer range to a maximum of ca. 19 Å in 10^{-6} s for the $Ru(4,4'\text{-}(COO_2R)_2bpy)_3^{2+}$ + TMPD reaction. For longer periods (e.g. ~ 1 s for organic triplets) distances of up to 30 Å can be obtained. For this situation, normal "Stern Volmer" excited state quenching (where $I_0/I \propto [Q]$) is not valid. Instead, $I_0/I \propto \exp[Q]$. Sample data for a random ensemble containing $Ru(bpy)_3^{2+}$* and MV^{2+} are presented in Fig. 6. As shown by Perrin, the slope of this curve gives a critical distance where $k(R) = 1/\tau_0$. Such static experiments only provide information of the rate at one fixed distance.

The value of the damping factor, α, can only be extracted from the time-resolved emission or absorption measurements. The theoretical description of donor decay for the case of energy transfer to randomly distributed acceptors in a matrix has been formulated by Inokuti and Hirayama [91]

$$\phi(t) = \exp(-t/\tau_0) \lim_{\substack{N\to\infty \\ V\to\infty}} \left[\frac{4\pi}{V} \int_0^{R_c} \exp(-tn(R)) R^2 \mathrm{d}R \right]^N$$

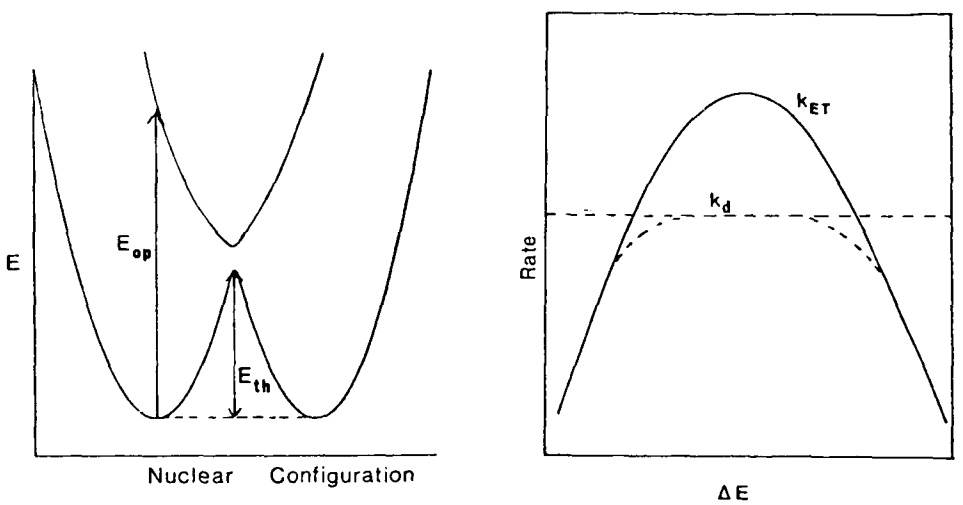

Fig. 5. Optical and thermal electron transfer processes. E_{op} represents the energy of an optical electron transfer (vertical process) from reactants to products. E_{th} represents the activation energy for a thermal electron transfer. Note, for $\Delta E = 0$, $E_{op} = E_{reorganization}$.

Fig. 6. Diffusional masking of very fast electron transfer reactions. Although the intrinsic transfer rate, k_{ET}, may be up to $\sim 10^{13}$ s^{-1}, observation may be limited by the collision frequency, represented hereby the horizontal line at k_d. Thus, a rate levelling effect is predicted until ΔE becomes very large.

where $n(R) = (1/\tau_0)\exp(\gamma(1 - R/R_q))$, $\gamma = 2R_q\alpha$ and R_q is the Perrin "critical" distance ($k(R_q) = 1/\tau_0$). The situation is entirely analogous for electron transfer. The essence of the problem is as follows: At $t = 0$, the emission probability is the same whether acceptors are present or not and $I_0/I = 1$. At short times ($t \ll \tau_0$), the emission probability in the presence of quencher is decreased due to the additional reaction pathway. At longer times, however, the number of donors with nearby acceptors has been depleted, leaving only donors with no close-lying acceptors. The probability of electron transfer for each of these pairs is small, and the decay approaches the rate in the unquenched system, resulting in a non-exponential decay curve.

Several groups [77–89,93] have reported data for such systems. Not only emission, calculating excited state survival, but also pulse radiolysis, calculating "anion" survival have been used for such studies. Studies of the relationship between ΔE and critical distances have resulted in important insight into the system dependence of α. As previously discussed, a simple barrier tunneling model predicts that rate (or R equivalently, R_c) should depend strongly on donor binding energy (B), since the exponential damping factor, α is proportional to $(B)^{1/2}$. By contrast, for superexchange, α is proportional to $\ln(\beta)$. In either mechanism, α is essentially independent of the acceptor energy.

Detailed studies of photoinduced electron transfer between $Ru(bpy\text{–}X)_3^{2+}$* and aniline derivatives in Lexan have shown that nearly identical R_c values (i.e. rate constants $k(R_c)$) are obtained at identical exothermicity, regardless of whether the donor energy or the acceptor energy is varied to adjust the exothermicity [203]. This result is not consistent with a barrier tunneling model, but is generally consistent with a superexchange mechanism. Independent detailed studies by Krongauz and Miller on electron transfer in MTHF glasses [204] have reached a similar conclusion. If these results are generally confirmed, they would explain why α seems nearly invariant over the many systems which have been examined, since α is presumed to depend only logarithmically on donor binding energy, or (equivalently) on medium conduction band energy. This point has been emphasized in a somewhat different context by Sutin [205], who noted that where $\Delta E > E_r$, the nuclear factor is optimized at large distance, while the electronic factor is optimized at small distance. This trade-off results in a maximum rate at $R > R_{\text{contact}}$. Values of α experimentally obtained at optimum ΔE range from 0.5 to 0.8 Å^{-1}, (i.e. $2\alpha = 1$–1.6) compared to the best theoretical guesses of 0.72 (Hopfield [39]), 1.3 (Jortner [40]) and 1.0 Å (Buhks and Jortner [46]). It should be stressed that α is expected to be somewhat system-dependent. There are several experimental difficulties encountered in studies of random ensembles. They include: (1) The reorganization energy depends on inter-

nuclear separation. Fortunately, this dependence is weak and is usually ignored [93]. (2) A more subtle and serious problem is that relaxations in glasses may occur during the time scale of observations, leading to time-dependent λ and ΔE values. (3) π–π interactions or Coulombic repulsion between acceptors can lead to non-randomized distributions. It is possible in some cases to correct for this with use of the appropriate distribution function [88]. (4) Likewise, ground state donor–acceptor complex formation can lead to complications. (5) The value of α is quite sensitive to the fit of the decay curve, so signal-to-noise ratios must be optimized, and several orders of magnitude in time must be explored.

A number of studies have also appeared on electron transfer involving reactants in micelles or vesicles [94–99]. These are interesting in themselves, but the dynamic nature of micelles, coupled with the uncertainty in the positioning (and partitioning) of any substrate, makes it difficult to extract any clearcut distance information. For example, an early observation of photoinduced long-range ET across a vesicle wall [98] was found to be in error, and the results were later attributed to photoinduced vesicular damage [99]. However, recent work by Hashimoto and Thomas [100] on micelles in frozen solution (77 K) is intriguing and the data generally agree with the distance scales found in homogeneous glasses. Finally, we should mention quite recent studies in diffusive solution, involving ligands which isolate donor and acceptor. Wherland has presented evidence for $k \propto \exp(-R)$ for Mn RCN exchange [225].

(ii) Bifunctional molecules

(a) Inorganic systems

The second class of experiments is concerned with electron transfer at a single, known distance. Perhaps the most widely investigated area in this class is that of charge transfer or intervalence bands [101–103] in bifunctional molecules [104–110] or biological partners [111–113]. An excellent review of early work in mixed valence chemistry is given by Robin and Day [101] (see also Hush [102,103]). In this section, we will be concerned entirely with molecular systems which have been designed explicitly to probe distance effects on the rate of electron transfer. The theory discussed in this review so far has dealt only with thermal electron transfer reactions. Even in cases where photoexcited states were involved, the actual electron transfer was a thermal process.

In typical bifunctional molecules, however, two possibilities exist. Thermal electron transfer can occur as before, in addition to the process shown in Fig. 5, optical electron transfer. This is an intramolecular charge transfer transition and corresponds to a change in the electronic density distribution

of the molecule. Such a transition is not a feature of the donor or acceptor alone, but only occurs only through their electronic coupling. These so-called "intervalence bands" typically fall in the near-IR region. The oscillator strength of the transition is related to the strength of interaction between the two functionalities [102,103].

The role of the intervening material in mediating this interaction has only recently been addressed. Ample evidence for electronic "conduction" through extended π-systems is available, and theoretical studies have suggested that both through-space and through-bond (sigma bond) pathways are possible [114,115]. Experimentally, elegant work by Stein and Taube [116,117] and Stein and coworkers [118,119] has shown that the theoretical models are at least qualitatively correct. Using a series of 2, 3, and 4 ring dithiospiro ligands as bridges between $Ru(NH_3)_5^{2+}$ and $Ru(NH_3)_5^{3+}$ moieties, they measured and compared the extinction coefficients of the intervalence bands. The decrease in electronic coupling (as measured by the extinction coefficients) through the series correlated well with the number of σ-bonds between metal centers [119].

Other evidence for through-bond interaction has been reported by Pasman et al. [120]. These workers used a number of different ligands in different conformations as bridges between organic electron donors and acceptors. A key observation is the presence of an intervalence band in (1)

(1)

while none was observed in the corresponding isomer (2).

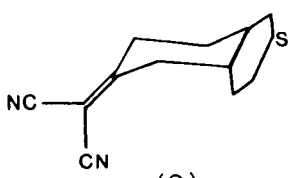

(2)

Through-space interaction is more likely in (2) than in (1) due to the smaller distance involved. Conversely, through-bond interaction is more likely for (1), since the stretched conformation allows for more efficient overlap through the σ-system [114,115]. Thus, the observation of an IV band for (1) only suggests that the through-bond interaction is more important than the through-space pathway for these compounds.

On the other hand, through-space interaction is implicated in the previously discussed matrix studies. In addition, Stein and Taube [116,117] have found evidence for its importance in several binuclear ruthenium complexes. In this report, the intensity of the intervalence band did not scale with the number of intervening σ-bonds, but rather the distance between ruthenium centers.

The relative contributions of through-bond and through-space interactions vary from system to system, and thus comparisons between non-homologous systems are difficult.

A considerable amount of work, most notably by Taube [104–108], has been done in an attempt to probe the electronic interaction in bifunctional systems. Rates of thermal electron transfer have been measured and properties of intervalence bands have been studied in an attempt to correlate the interaction energy with various structural parameters.

Let us consider a system consisting of a donor moiety, an acceptor moiety, and a series of closely-related linkages designed to attach covalently donor to acceptor with a variety of separation distances. We assume that ΔG_{rxn} and the Franck–Condon factors involved are constant.

Since the electronic coupling decreases exponentially with distance, we would expect the oscillator strength of the IV band to behave similarly. However, in the limit of all reactions being adiabatic, the rates of thermal electron transfer would be identical (provided, of course, that the interaction did not grow large enough to decrease the activation barrier appreciably). In all cases, the "transmission coefficient", κ, would be unity. Since the Franck–Condon factors are constant, the rates would not vary. Only in the case of weak electronic coupling, that is, nonadiabaticity, would the rate depend on donor–acceptor distance. Thus, both optical and thermal measurements are necessary to provide information about the electronic coupling in these systems.

Taube and coworkers [108] have extensively studied Co(III)–Ru(II) and Ru(II)–Ru(III) systems. Often, however, the set of systems for which thermal rates could be measured was orthogonal to the set for which IV transitions could be found [108].

Recently, Richardson and Taube [107] have reported an extensive study of complexes of the general formula $[(Ru(NH_3)_5)_2L]^{n+}$ ($n = 4, 5, 6$) where L is a rigid bifunctional organic bridging ligand. Some 14 ligands were examined, and all but two exhibited an intervalence band in the near IR for the Ru(II)–L–Ru(III) state. In general, the metal–metal interaction decreased exponentially with the number of conjugated atoms, as expected [121]. However, the complexes are divided into two groups, those with an even or those with an odd number of atoms between metal sites. Thus, ligands with an even number of conjugated atoms between metals showed greater

metal–metal interaction than those with an odd number. The slopes of the two lines in a plot of $\log(H_{ab})$ vs. number of total conjugated atoms were the same. The results were explained through back-bonding and charge density effects.

Further, they calculate that all ligand π and π^* ligand orbitals contribute significantly to the metal–metal electronic coupling, rather than only the LUMO (or HOMO), as earlier assumed. However, if one orbital lies particularly close in energy to the metal orbitals (e.g. this can be the case for delocalized organic ions), it may dominate the contributions to coupling [107]. Very recent theoretical work concerning the orbitals involved in coupling has been provided by Stein and coworkers [119] and Beratan and Hopfield [122].

Other species under investigation include Ru(III)–Cu(I) and Co(III)–Cu(I) bifunctional molecules [109,110]. An interesting report from Hurst and coworkers [110] involves

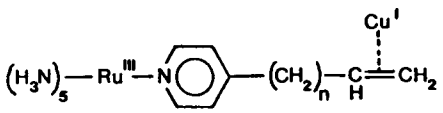

When $n = 0$ both thermal and optical electron transfer can occur. When $n = 2$, 3, 4, or 7, one might expect the molecule to fold over, with the overlap of the alkene bond and the pyridine moiety providing efficient electronic interactions. However, no IV band is seen and the electron transfer rate is strictly second order (intermolecular). Thus, for this system, at least, overlapping π-orbitals do not provide an efficient pathway for electron transfer. This may have important biological implications. In few systems have IVCT bands been directly compared with thermal rates. Recently, Haim [113] studied Co(III) complexes were k predicted by IVCT $\gg k_{obs}$. Clearly more such studies would be useful.

Compared with work on IV systems, very little work has been carried out on fixed distance thermal electron transfer in bimetallic systems. However, several quite recent studies are noteworthy.

Iseid and coworkers have reported intramolecular electron transfer in Co(III)–peptide–Ru(II) systems [206]. Unfortunately, the rates observed in these systems are very slow (reflecting the large inner sphere reorganization energy of Co(III/II). This sluggish rate affords sufficient time for large-scale librational motion of the peptide spacer, thereby obscuring the validity of the "distance".

A more rigid system has been studied by Anderes and Lavallee [207a]. While no absolute rate is assigned, it is intriguing that the hydrocarbon spacer reduces k_{et} relative to the collisional rate: $t_{1/2}$ (collisional)/$t_{1/2}$

(intermolecular) is greater than 10^3! Related work by Geno and Dawson led to a similar conclusion [207b].

A quite interesting comparison between "homogenous" fixed-distance electron transfer and heterogenous fixed distance transfer at an electrode comes from the work of Li and Weaver [208] on modified gold electrodes. Electrodes were coated with complexes of the general form $L_5Ru\text{-}L^{-S-}$ where the thioether tightly binds to Ru to give a packed monolayer. (In such a monolayer, the C chain is largely extended. For equivalent work on photochemical ET in extended monolayers, the papers of Kuhn and Mobius should be consulted [209]). Weaver et al. find that k_{et} is proportional to $\exp(-\alpha n)$ (i.e. $\exp(-\alpha R)$) where $\alpha \sim 1.2$ Å^{-1}.

Major work has appeared within the past two years on bichromophoric porphyrin compounds, particularly porphyrin quinone adducts.

Independently Chang, Wasielewski, Moore, and co-workers [210], have prepared and characterized photoactive metalloporphyrin quinone adducts. One important result of this work is that very rapid photoinduced charge separation ($\sim 10^{11}$ s^{-1}) can be observed when the reaction exothermicity is optimized. An exciting corollary to this work is the production of trichromophoric systems of general structure donor–porphyrin–acceptor [209,210]. In two such systems, rapid electron transfer occurs between porphyrin and acceptor. The resulting radical pair can recombine, with no net energy storage. However, electron transfer may occur between the secondary donor and porphyrin cation radical in competition with the unproductive back recombination. As a result, an electron-hole pair is created (donor + acceptor) separated by an "insulating" porphyrin. Thus, back reaction is strongly impeded, (by a factor of more than 10^6) and $k_b \leqq 10^6$ s^{-1} [210]. Finally, we note that in the reactions studied by Wasielewski, k_b is less than k_f reflective of apparent exothermically restricted kinetics.

Loach and coworkers [130,131] have synthesized several covalently-linked porphyrin complexes. For some solvents, at least, the fluorescence lifetimes are shorter for the porphyrin–quinone than either the porphyrin or the porphyrin-reduced quinone species. This is taken as evidence for an intramolecular electron transfer involving the porphyrin singlet state. Fluorescence yield measurements and EPR data are also presented as evidence.

Finally, we consider recent work on bichromophoric systems by Closs and Miller [211]. Using steroid spacers, these workers demonstrated that rapid ($> 10^8$ s^{-1}) long distance electron transfer could occur at closest contact distances > 10 Å. A striking result of this work is the unambiguous demonstration of exothermic rate restriction (i.e. "inverted behavior") in the linked systems, but not in analogous diffusional reactions. This point is discussed in more detail in the section dealing with the "inverted region".

(b) Biological electron transfer

Much of this work on these relatively simple inorganic systems has been paralleled in the field of biochemistry. For example, by looking at transient changes in the Soret region (400–450 nm) upon illumination in the near-IR, Hopfield and Potasek found very weak CT transitions in the cytochrome c-cytochrome c peroxidase [111] and cytochrome c-hexacyanoiron system [112]. However, according to a later report [123], this interpretation may be incorrect.

Gray and coworkers [125–128] have done a considerable amount of work on electron transfer between proteins and small inorganic complexes. In one report [125], the reactions of cytochrome c (horse heart) with $Fe(EDTA)^{2-}$, $Co(phen)_3^{3+}$, $Ru(NH_3)_6^{2+}$ and $Fe(CN)_6^{3-}$ were investigated. The rates were corrected for work terms and values for the protein self-exchange rate, k_{11}, were estimated from the Marcus cross-relation. They found that these values varied by a factor of about 10^3 for the various reactants in the order

$$Fe(CN)_6^{3-} > Co(phen)_3^{3+} > Ru(NH_3)_6^{2+} > Fe(EDTA)^{2-}$$

This was attributed to differences in the penetration of the protein surface and differences in the degree of π-overlap between redox centers.

In another report, Mauk et al. [126] developed an equation for the reaction distance in a protein self-exchange reaction:

$$R_p = 6.2 - 0.35 \ln(k_{11}^{\infty}) \tag{13}$$

where R_p = half the intersite distance for protein self-exchange and k_{11}^{∞} is the calculated self-exchange rate, extrapolated to infinite ionic strength. It should be noted that this equation is valid only when the inner-sphere reorganization term is small. A number of experiments involving inorganic reactants and different proteins were performed to test the model. Distances on the order of 10 Å (heme center-to-iron center) for the reaction of cytochrome c with $Fe(CN)_6^{4-}$, a typical reagent, were calculated.

A particularly promising approach to understanding fixed site ET in proteins is based on "coordination chemical modification". In this vein Winkler et al. [127a] and Isied and coworkers [127b] recently reported the attachment of a $Ru(NH_3)_5^{n+}$ ($n = 2, 3$) group to the histidine-33 residue of ferricytochrome c. The protein can effectively quench the emission of $Ru(bpy)_3^{2+}$* through an electron transfer mechanism. When the $Ru(NH_3)_5^{n+}$ is present in the +3 state, the electrons transferred to the modified protein partition between the Ru and Fe. The Ru(II)–Fe(III) species thus created can undergo a thermodynamically downhill ET reaction to Ru(III)–Fe(II). This has been shown to occur with a rate constant $k_{ET} = 30 \pm 5\ s^{-1}$. The shortest (His-33)–(heme) distance is 10 ± 1 Å. Considering this separation, the measured rate is reasonable for a reaction which is only modestly

exothermic ($E^0(Fe^{III}/Fe^{II}) - E°(Ru^{III}Ru^{II}) = 0.11$ V). The observed temperature independence (from 0 to 37°C), was originally interpreted as suggesting a small reorganizational barrier. Subsequent careful work by Nocera et al. [129a] and independent work by Isied et al. [129b] suggest E_r is approximately 0.8 ± 0.2 V.

EPR data may be of interest in estimating electronic coupling. Leigh et al. [132] report that photodissociation of CO from cytochrome a_3 in cytochrome c oxidase causes some of the associated cytochrome a to convert to high spin, even at 10°K. Although the low to high spin conversion is largely prevented at low temperature, the fact that it occurs at all indicates that the cytochrome a_3 and cytochrome a may be quite close together.

In a very elegant study, Okamura et al. [133] also rely on EPR data to support their three step model of ET in the reaction centers of *R. sphaeroides*. They also note that the exchange interaction from the EPR data, J, is related to the electronic coupling matrix element, H_{ab} by the expression

$$J/2 = -|H_{ab}|^2/(E_A - E_B - \Delta) \tag{14}$$

One can also obtain an expression for the ET rate in terms of J

$$k_{ET} = |J|/2h\left(\frac{\pi E_a}{kT}\right)^{1/2} \exp(-E_a/kT) \tag{15}$$

k_{ET} and $|J|$ are both measurable quantities, and thus a theoretical value for E_a can be calculated. In addition, these workers determined E_a empirically from the temperature dependence of the decay time. The agreement between these two values is excellent; E_a (exp) $= 0.67 \pm 0.03$ eV and E_a (calc) $= 0.61$ eV.

These results support current tunneling theories of ET reactions. The system appears to be nonadiabatic and the estimated separation of the redox centers is 7.5 to 10 Å, depending on the exact model used.

Finally, the NMR of cytochrome c–cytochrome c peroxidase (horse, Type VI) has been studied by Gupta and Yonetani [134]. From the lack of interaction, they conclude that the heme–heme distance is greater than 25 Å. Still, electron transfer in this complex is relatively facile, proceeding with a rate constant $k = 2 \times 10^3$ s^{-1} for the reaction Fe(IV) ccp: Fe(II)cyt c → Fe(III)ccp: Fe(III)cyt c ($\Delta E \sim 0.9$ V). Recent studies of a lower exothermicity reaction Fe(II)ccp: Fe(III)cyt c → Fe(III)ccp: Fe(II) cyt c) ($\Delta E \sim 0.4$ V) show a dramatic rate decrease: $k_{et} \sim 0.2$ s^{-1}!

Quite recently, general studies have appeared in which the Fe porphyrin active site in a heme protein has been substituted by a redox photoactive Zn(II) porphyrin. In a prototype study, Hoffman and coworkers [124] reported on photoinduced electron transfer from Zn(II)porphyrin to Fe(III)porphyrin in a hemoglobin derivative, α_2Zn(II) → β_2Fe(III).

Zn(II)porphyrins are substituted into the α subunits of the hemoglobin tetramer, while Fe(III)porphyrins are retained in the β subunits. Photoexcitation yields the Zn(II)porphyrin triplet state, which decays by electron transfer, ($k_{et} = 100\ s^{-1}$) to reduce the β site Fe(III)porphyrin to Fe(II). The back reaction α(Zn(II)α(porphyrin$^{\cdot+}$)β Fe(II)β Fe(III) $\rightarrow \alpha_2$Znporphyrin β_2Fe(III)porphyrin is partially precluded by a rapid intramolecular degradation reaction of the (Zn porphyrin)$^{\cdot+}$ cation radical.

A key finding of this work was that electron transfer could occur relatively rapidly (60 s^{-1}) over a crystallographically-characterized long distance (20 Å closest approach between the porphyrins). Quite recently, these workers reported detailed studies of the dependence of rate on temperature [212]. In common with the Chance–DeVault study, activated behaviour ($E_{act} \sim 3$ kc M^{-1}) was observed at high temperature, while a temperature-independent plateau was found at low temperatures. Using the previously discussed model of Hopfield, and the observed "critical temperature" for onset of activated rate behaviour, the authors derive an (average) frequency of 400 cm^{-1}, and a reorganization energy of ca. 2.5 eV. This latter value appears striking in light of the many suggestions that biological reorganization energies should be intrinsically low (reflecting, for example, a presumed low local dielectric constant in the surrounding protein). Independent and simultaneous work on physiological donor–acceptor pairs has been reported by McLendon et al. [213]. These authors have reported studies of photoinduced electron transfer involving metal-substituted Zn(II) cytochrome c [214] and Zn(II) hemoglobin [215], both of which can transfer an electron to a common physiological partner, cytochrome b5.

As shown in Fig. 7, the heme active sites are well separated (10 Å; edge–edge) in these physiological adducts. However, the donor–acceptor distance in the Zn(III)Hb/Fe(III)b5 system is shorter in αZn(III) βFe(III) hemoglobin. In light of the previous discussion, a faster rate is anticipated for the Zn Hb/b5 system and this is observed: $k_{et} = 6 \times 10^3\ s^{-1}$ for electron transfer from Zn(II) Hb to Fe(III) cyt b5 within the specific, noncovalent complex formed by these proteins.

However, a surprising result is found for electron transfer from Zn(II) cyt c to Fe(III) cyt b5 [215]. Cyt c/cyt b5 form a strong specific noncovalent complex which is believed to be strongly homologous to the Hb/cyt b5 complex [216]. The active site separation (10 Å) orientation (parallel hemes) and intravening protein media are very similar for both the Hb/cyt b5 and cyt c/cyt b5 couples. Nonetheless, photoexcited ^{3}(Zn(II)cyt c) transfers an electron to cyt b5 with $k_{et} = 3 \times 10^5\ s^{-1}$. This rate is 500 times faster than the corresponding rate for the cyt b5 system! It is clear that nature is a more subtle designer than might be anticipated from the small molecule studies discussed thus far.

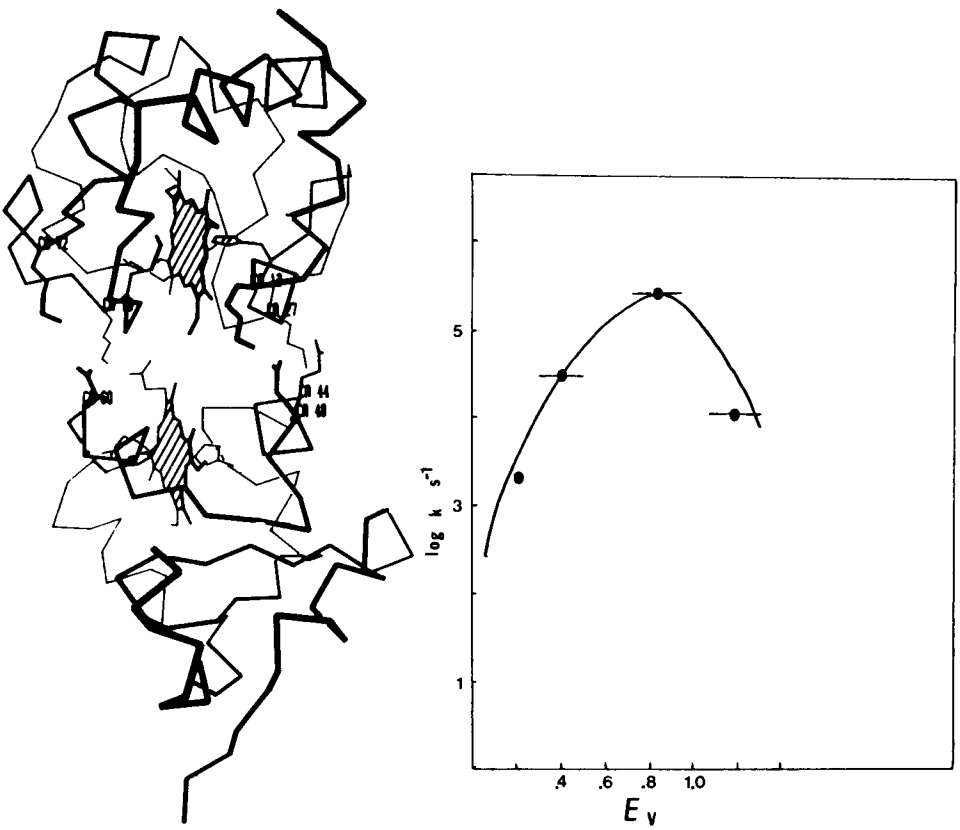

Fig. 7. Proposed structure of the cytc/cytb5 complex (courtesy T. Poulos, Genex). Closest heme-heme distance is ca. 8 Å.

Fig. 8. Plot of rate vs. ΔG for a series of metal substituted cytc/cyt b5 complexes.

The c/b5 system offers a particularly useful model for testing the dependence of intraprotein electron transfer rates on ΔE. One result of such studies [215] is presented in Fig. 8. From this work, it appears that $E_r \sim 0.8$ V, much higher than anticipated by theorists [218] who assume a minimal ($\epsilon \approx 2$) protein dielectric. It is not clear where the theoretical calculations err [219]. However, in the few cases so far examined, E_r is invariably large for protein–protein couples. Understanding and extending these results should pose interesting problems for theorists and experimentalists alike.

The few studies thus far reported in structurally characterized biological systems are compiled in Table 2. Initially some aspects of these studies seem confusing. For example, in the Fe(III)cyt c–His33–Ru(II)$(NH_3)_5$ derivative, the electron transfer occurs over a nominal distance of 10 Å, comparable

TABLE 2

Some rates of intramolecular biological electron transfer reactions

System	E^0	R(Å)	k(s^{-1})	Ref.
$Fe^{II}cytb_5/Fe^{III}cytc$	0.2	8 [a](16)	1.5×10^3	[b]
$^3Zncytc^*/Fe^{III}b_5$	0.8	8	3×10^5	
$^3H_2porfc^*/Fe^{III}b_5$	0.4	8	1×10^4	
$Zncytb_5/Fe^{III}cytc$	1.1	8	4×10^3	
$H_2porfc^-/Fe^{III}b_5$	1.1	8		
$Fe^{III}b_5/Fe^{III}Hb$	0.05	8(16)	0.01	[c]
$ZnHb/Fe^{III}b_5$	0.9	8	8×10^3	[d]
$Znb_5/Fe^{III}Hb$	1.0	8	2×10^3	[e]
α Zn β $Fe^{III}Hb$	0.9	20	100	[e]
$Fe^{IV}ccp(ES)/Fe^{II}cytc$	0.9	16(24)	2×10^3	[f]
$ccp(ES)/Zn^{II}cytc$	0.4	16	2	[g]
$ccp(ES)/H_2porfcytc$	0.1	16	4×10^{-3}	[g]
$Fe^{II}ccp/Fe^{III}cytc$	0.4	16	0.25	[h]
$Fe^{III}ccp/porfcytc^-$	1.0	16	180	[h]
ccpES/protein radical (TRP)	0.1	?	0.1	[i]
$^3Znccp^*/Fe^{III}c$	0.8	16	200	[i]
$Fe^{II}cytc_1/Fe^{III}cytc$	0.1	?	50 [j]	[j]
$Fe^{II}cytc/cyt$ oxidase	0.1	12(20)	> 700	[k]
cyt c_3 (D. Gigas)	0.06	4	$>10_4$ [l] *flavo cytc* 553 (*flavin* + *heme*)	10^{3m}
Ruthenium substituted proteins				
$(NH_3)_5Ru$ His 33 cytc	0.15	11(17)	40	[n]
$(NH_3)_5Ru$ His azurin	0.2	10	2.5	[o]
$(NH_3)_5Ru$ His Mb	0.05	13(18)	0.02	[p]
$(NH_3)_5Ru$ His ZnMb	~ 0.8	13	2×10^3	[q]

[a] Number given is closest edge—edge distance ((Fe–Fe) center–center distance).

[b] G. McLendon and J.R. Miller, J. Am. Chem. Soc., 107 (1985) in press.

[c] G. McLendon, J.R. Miller and A.G. Mauk, to be published.

[d] K. Simolo, A.G. Mauk, M. Mauk and G. McLendon, J. Am. Chem. Soc., 106 (1984) 5013.

[e] S. Peterson-Kennedy, J. McGourty and B. Hoffman, J. Am. Chem. Soc., 106 (1984) 5010.

[f] T. Yonetani.

[g] K. Taylor and G. McLendon, J. Am. Chem. Soc., submitted.

[h] K. Taylor, E. Chaung, A. English, J. Miller and G. McLendon, Proc. Nat. Acad. Sci., in press.

[i] P. Ho, G. Sutoris, N. Wang, E. Margolish and B. Hoffman, J. Am. Chem. Soc., 107 (1985) 1070; B. Hoffman, P. Ho, Soloman, K. Kang and E. Margolish, Biochemistry, 23 (1984) 4122.

[j] Evidence suggests the rate is limited by a conformational change.

[k] M. Cusanovich and G. Tollin, Biochemistry, 21 (1982) 3122.

[l] H. Sautos, I. Moura, J. Legall and A. Xavier, Eur. J. Biochem., 141 (1984) 283.

[m] M. Cusanovich and G. Tollin, Biochemistry, 21 (1982) 842.

[n] D. Nocera, J. Winkler, K. Yocum, E. Bordignon and H. Gray, J. Am. Chem. Soc., 106 (1984) 5145; S. Iseid, C. Kuehn and G. Worosila, J. Am. Chem. Soc., 106 (1984) 1722.

[o] N. Kostic, R. Margolish, C. Che and H. Gray, J. Am. Chem. Soc., 105 (1983) 7765.

[p] R. Crutchley, W. Ellis and H. Gray, J. Am. Chem. Soc., in press.

[q] A. Axup, R. Crutchley and H. Gray, to be published.

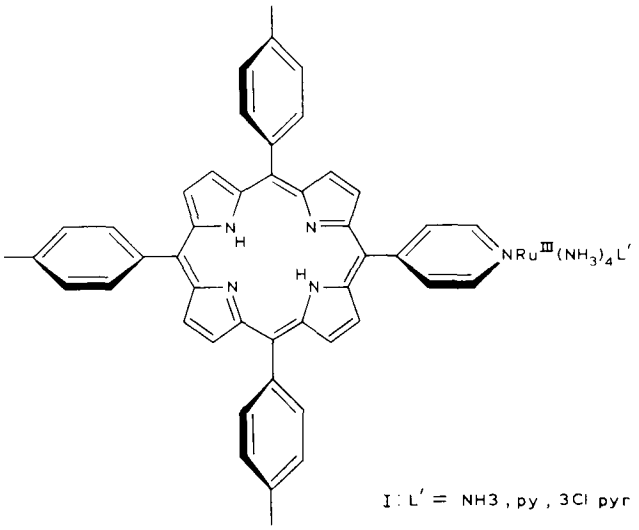

Fig. 9. General formula of a new class of bifunctional porphyrin-Ru(III) ammine complexes.

with that in the Zn(II)cyt c/cyt b5 system. However, electron transfer from His33–Ru(II)$(NH_3)_5$ to the cyt c heme occurs with a rate $k_{et} \sim 30\ s^{-1}$, while transfer from ^{3}(Zn*cyt c) to Fe(III) cyt b5 occurs with $k_{et} > 10^5\ s^{-1}$. Does this enormous rate difference over the "same" distance disprove the theories discussed? In fact, much of this rate difference may be anticipated.

A subtle problem in the definition of "distance" may contribute to such rate differences. When an electron is transferred from Ru(II), is the appropriate distance the 10 Å closest contact distance from His33 to the porphyrin edge, or is it the more than 16 Å distance from the Ru atom to the Fe atom? The shorter "ligand–to–ligand" distance is likely to approximate closely the actual "through-space" distance of the electron transfer process. However, this approximation is not rigorously correct, since the wavefunction of the electron donor is largely localized on the Ru(II) metal center. Delocalization to the "closest contact" imidazole of Ru is incomplete. Thus electron transfer from the imidazole site might best be "down-weighted" by the (percentage excess) electron density at that site. Some support for this idea comes from studies by Franco et al. [220] who have prepared porphyrins substituted by Ru(III)$(NH_3)_5$ pyridine (Fig. 11). Studies of these molecules show that even when exothermicity is optimized, the electron transfer rates for the Ru derivatives are far smaller than for homologous quinone or viologen adducts. The simplest explanation for this difference is that electron transfer to the organic acceptors is adiabatic, but transfer to the Ru derivative is nonadiabatic, consistent with poor porphyrin–Ru overlap. If

this observation and explanation can be generalized, then the appropriate distance for electron transfer in substituted cyt c is $R \sim 16$ Å.

Another aspect of the dependence of rate on distance may be peculiar for proteins. Consider the dependence of rate on distance, as embodied in the superexchange model already discussed. For any "normal" ensemble, (i.e. a Euclidean embedding space) the number of superexchange couplings will be directly proportional to the donor–acceptor distance. However, perhaps proteins are not Euclidean objects? It has shown [221] that for spin exchange, coupling occurs as if proteins have a reduced dimensionality; i.e. site occupancy is proportional to $R^{1.4}$, not R^3! Such "fractal" dimensionality commonly occurs for highly complex, tortuously twisted structures (like proteins). Spin exchange is, of course, highly analogous to electron exchange. It may prove interesting to determine whether the "fractal" dimensionality of proteins is important in the context of protein electron transfer reactions. If so, a weaker distance dependence might be observed for protein electron transfer than for electron transfer involving equivalent donors and acceptors in a conventional solvent. Another final possible contributor to rate differences in various protein derivatives may arise from the dependence of rate on donor electron binding energy. For barrier tunneling, a shift in binding energy from 3 V for Ru to 1 V for ^{3}(Zn(II)porphyrin)* would result in a rate change by a factor of more than 100. However, the previously cited studies which show a weak dependence of rate on binding energy cast doubt on this possibility.

Several points in the Table merit particular attention. First, almost all the studies cited are less than two years old. Second, at equivalent distances, rates are quite sensitive to exothermicity. Finally, the unimolecular rates observed under conditions of complete complex formation are significantly slower than anticipated from the bimolecular rate constants. Furthermore, the bimolecular binding constants inferred from steady state measurements are far higher than equilibrium binding constants measured under equivalent conditions. These observations together suggest that there are underlying mechanistic complications in these protein–protein electron transfer reactions.

I. INVERTED REGION

Both classical and quantum mechanical theories of electron transfer predict a rate fall-off at very large ΔE. Simple Marcus theory [1–10], for example, predicts a quadratic dependence (with a maximum at $\Delta E = E_r$) since $E_{act} = (\Delta E - E_r)^2/4E_r$ (equation (5)).

Later quantum theories [38–56], accounting for nuclear tunneling and reaction into excited vibrational states of the product, predict a slower

fall-off with ΔE. This effect can be qualitatively discerned by looking at Fig. 4. The nuclear barrier is thinner in the "inverted" region ($\Delta E > E_r$) than in the "normal" region. Hence, nuclear tunneling makes a larger contribution to the rate in this region, leading to slower drop-off. Despite these predictions, the experimental evidence for inversion was quite sparse until recently [71,135–148].

A fairly common observation in diffusional systems is that rate "levels off" at high ΔE. This was reported, for example, in the pioneering study of Rehm and Weller [145]. They [145,146] and others [71,135–144,147,148] have attempted to fit the data using empirical free energy relationships. Of course, without understanding the relevant chemistry, the value of such empirical relationships is questionable.

There are several explanations for the lack of inverted behavior. These include:

(1) Formation of excited state products. When ΔE is very large, the product can often be formed in an electronically excited state. This opens a new reaction channel with a less favorable ΔE (and hence faster theoretical rate). In fact, the mere formation of excited products has been taken as evidence for inversion [149,150].

(2) Formation of vibrationally excited products [150–152]. Arguments here are similar to those in (1).

(3) An increase in H_{ab} as ΔE increases. Although the value of the nuclear term is predicted to decrease in the inverted region, the electronic term may increase. This occurs because the barrier height, V (see equation (6), Fig. 2), decreases as ΔE becomes large. The magnitude of this effect is uncertain. However, it should only occur in systems involving nonadiabatic ET. (Rates of adiabatic reactions do not depend explicitly on H_{ab}.)

(4) Diffusional masking. When the electron transfer rate in the precursor complex becomes very fast, it is no longer the rate limiting step. Rather, the diffusion of the two reactants to form the complex is the slow step. Thus, one cannot detect a rate drop-off in such a system until k_{ET} drops to a value less than k_{diff} and a "leveling off" is observed (see Fig. 6). This effect is amplified by the distance dependence of electron transfer. At high ΔE, reaction can take place over large distances. This effect modifies the conventional diffusion theory, and in effect results in a particularly wide diffusional masking regime. Recent discussions of this diffusional complication with supporting data can be found in work by Mauzerall [223], Sutin [205], and Miller et al. [156]. Because of these difficulties, examples of inverted behavior in solution reactions are quite rare.

One apparent example of inversion in solution involves quenching of $Ru(LL)_3^{2+}$ (LL = 2,2′-bipyridine or 4,4′-dimethylbipyridine) by $M(LL)_3^{3+}$ complexes (M = Ru, Os, or Cr) as reported by Creutz and Sutin [153].

However the inversion here is much smaller than that predicted by theory. The inverted region was also implicated in the reaction of e_{aq}^- with $Ru(bpy)_3^{3+}$ [154]. In this work, it was found that nearly all of the reaction produced excited states of $Ru(bpy)_3^{2+}$ ($\Delta G_{reaction} = -1.93$ V for CT $Ru(bpy)_3^{2+}$) rather than the ground state ($\Delta G_{reaction} = -4.0$ V).

Complications due to the formation of excited state products can be avoided by studying systems which lead only to products with no low-lying electronic states.

The problem of diffusional masking can be eliminated by working in a rigid matrix. Indeed, some of the best evidence for inversion comes from the pulse radiolysis studies of Beitz and Miller [77,156], who observed a rate reduction of more than 10^5 between $\Delta E = -1.1$ V and $\Delta E = -3.0$ V. These workers studied electron transfer to various electron acceptors in 2-methyltetrahydrofuran (MTHF) at 77 K. By measuring the survival probability of a trapped electron vs. time, they found relative rates of electron transfer for a long list of acceptors. Benzonitrile ($\Delta E = 1.1$ V) had the fastest rate, while the relative rate for benzoquinone ($\Delta E = 3.0$ V) was 3×10^{-6} (compared with benzonitrile). By considering the formation of excited states for some acceptors, the scatter in their data is greatly diminished, and an "inverted region" is implied. It is possible that differences in the reorganization energies of each species could shift some of the points around, but it is unlikely that there would be any great differences. Thus, these data, at least qualitatively, point to inverted behavior.

One problem in studies using matrices has been briefly addressed by both experimentalists [155,156] and theoreticians [157–159]. This is the necessity of considering not only the energetics of solvent reorganization, but also the dynamics. If the solvent cannot completely reorganize during the time frame of an experiment, the product remains in an unfavorable environment. Van Duyne and Fischer [159] contend that this corresponds to a decrease in reaction exothermicity. Hence, ΔE depends on the degree of solvent relaxation and is a function of time. Alternatively, the increase in viscosity can be considered to cause a change in the medium reorganizational energy. In any event, since there are many different reorganizational modes, all with different relaxation rates, the situation can become quite complex.

Another way to avoid diffusional masking is through studies of bifunctional molecules, similar to the linked donor–acceptor systems mentioned earlier (distance dependence section). The only difference here is the use of a single linkage with substitution of various closely related donor–acceptor pairs to alter ΔG. Many of the synthetic and experimental problems discussed earlier apply here, although some are less serious, since only relative rates are important and parameters such as absolute distance need not be known (so long as they remain constant for all donor–acceptor pairs.)

Strictly speaking, the various donor–acceptor pairs should be as homologous as possible in order to ensure that all parameters (e.g. E_r, H_{ab}, R) remain relatively constant.

A very interesting experiment which avoids comparisons in a series of compounds has recently been performed by Miller [160]. The principle behind this experiment is that the onset of inversion depends not only on ΔE, but on the relative magnitudes of ΔE and E_r (eqn. 5). Thus, one should be able to detect inversion by simply changing solvents (and hence E_r) while keeping the reacting partners unchanged.

Miller's system consisted of a biphenyl moiety and a 1,4-benzoquinone moiety separated by a rigid steroid bridge. Using pulse radiolysis, a charge could be created on either end of the molecule. When the biphenyl group was initially reduced by the pulse, a secondary reaction was observed. This corresponds to the very exothermic ($\Delta E = 2.0$ V) transfer of the excess electron from biphenyl to the quinone group. It was found that the driving force was identical in the solvents 2-methyltetrahydrofuran (MTHF) and isooctane. On the other hand, E_r is expected to be much smaller in isooctane than in MTHF due to the lower polarity of the former. Thus, if the reaction is inverted, it will be slower in isooctane than MTHF. This is exactly what Miller observes, the measured half-lives being 7 ns in MTHF and 400 ns in isooctane [160].

Other data supporting inversion have been reported in reactions of anion radicals [161] or hydrated electrons [162] with micelle-trapped organic molecules. Unfortunately, ΔE values in these systems are relatively uncertain.

In conclusion, while inversion is rare in collisional reactions, due to diffusional masking, strong evidence exists for inversion where donor–acceptor distances are fixed.

An interesting application of kinetic inversion has been reported by several groups studying photoinduced change separation in porphyrin quinone systems [210]. In one elegant study Wasielewski showed that when ΔE for back reaction was far greater than both ΔE for the forward reaction and E_r, then $k_f > k_b$ [210b]. This happy circumstance allows design of trichromophoric systems which produce long-lived charge separation.

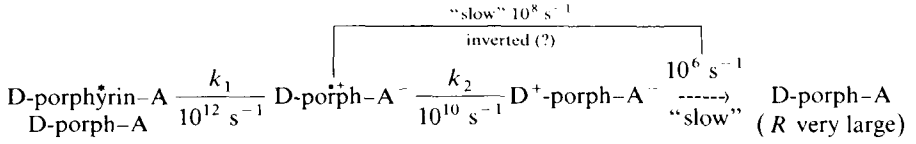

J. TEMPERATURE STUDIES

As mentioned previously, quantum effects can be expected to manifest themselves in the temperature dependence of ET rates. Activated behavior at

higher temperature, coupled with activationless behavior at lower temperature is highly suggestive of nuclear tunneling.

Let us first explain events which occur during photosynthesis. The bacterial photosynthetic reaction center consists of the following parts (we borrow the notation of DeVault [11] for clarity):

p—primary electron donor, a dimer of bacteriochlorophyll (BCh1);
I—intermediate electron acceptor;
A—"primary" electron acceptor, possibly an iron-quinone complex;
Q—secondary electron acceptor, a quinone;
C—secondary electron donor, a cytochrome.

There may be several types of species Q and C involved.

The system can be thought of as originating in the state $C \cdot P \cdot I \cdot A \cdot Q$ with the following reaction sequence:

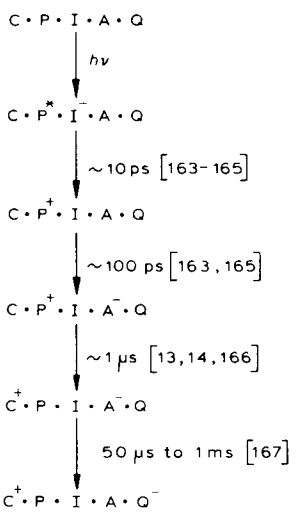

Green plants have two photosystems, PS-I and PS-II, which will not be discussed here. It will suffice for our purposes to note that the green plant photosystem I is similar to the bacterial photosystem. More detailed information can be found in works by DeVault [11], Govindjee [168] and Barber [169].

To date, many biological systems which exhibit low temperature rate-levelling effects have been studied. Some early reports of this effect arise from the work of Chance and Nishimura [170], DeVault and Chance [13], and DeVault et al. [171].

The particular reaction studied in these early reports was the reduction of the primary electron donor by the secondary electron donor, or the step

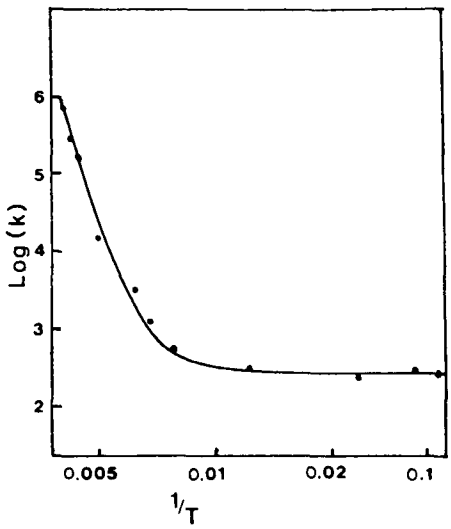

Fig. 10. Temperature dependence of the cytochrome oxidation in *C. vinosum*. This figure is adapted from ref. 11.

$C \cdot P^+ \rightarrow C^+ \cdot P$ in the sequence above. Generally, the rate was measured through detection of the oxidized cytochrome.

Chance and Nishimura [170], working with *Chromatium*, observed photo-induced oxidation of cytochrome at both 300°K and 80°K. The total absorbance change was less at 80°, (although still quite substantial), but the reaction half-time was unchanged. The subsequent dark reaction, re-reduction of the cytochrome, occurred only at 300° and was completely absent at 80°K. Later results of Chance and coworkers [13,171] provided full rate vs. temperature data down to 4.4 K (Fig. 10). The data correspond to an activation energy above 130 K of 3.3 kcal mol^{-1}, while for T of less than 100°K, $E_{act} \leqq 4$ cal mol^{-1}. These coworkers contend that the slowness of the reaction indicates the existence of a barrier, while the lack of activation energy (at low temperature) indicates that the system does not pass over the barrier classically.

Chance et al. [13,171] suggested that an electron tunneling mechanism was operative. Subsequent discussion in the literature focused on the height of the barrier, its physical meaning, and the distances over which an electron could travel. Following earlier suggestions of Levich and Dogonadze [36] and Sutin [8], it gradually became clear that nuclear tunneling rather than electron tunneling, was responsible for the temperature independence. While the electron may be tunneling, its behavior does not affect the temperature dependence of the rate. As previously mentioned, the electron may tunnel only between isoenergetic states. Since this occurs only in the vicinity of the

crossing point in Fig. 1 (which represents nuclear positions) it is obvious that nuclear motion must accompany electron transfer. Further, it is likely that this nuclear motion controls the temperature dependence of the rate. The activationless portion of the plot is attributed to the fact that this nuclear motion may occur by (nuclear) tunneling, and this process is essentially independent of temperature.

In *C. vinosum*, there are two types of cytochrome which can normally donate electrons to P^+. However, only the "low-potential cytochrome" (more easily oxidized) was found to react at low temperatures [172,173].

Although *C. vinosum* exhibits cytochrome oxidation even down to 4 K, *R. sphaeroides, Rhodospirillum rubrum*, and *Rhodopseudomonas capsulata* do not undergo this reaction at 77 K [11]. Kihara and Chance [14] have reported a number of species which do exhibit cytochrome oxidation at 77 K. Unfortunately, however, they did not report any quantitative data concerning the temperature dependence of the rate.

In other studies, cytochrome oxidation is shown to occur at low temperature, and full rate vs. temperature data is provided. As in *C. vinosum* [13] the low-temperature branch of the plot often indicated a negligible activation barrier at temperatures below 140 K. Reports include those of Seibert and DeVault [174], Dutton et al. [30], and Kihara and McCray [175].

K. REVERSE REACTION

When the secondary acceptors (quinones, Q) or secondary donors (cytochromes, C) are removed (or otherwise deactivated) from a biological system, a frequent observation is the lack of long-lived charge separation. The state transiently produced, $P^+ \cdot I \cdot A^-$, returns to the ground state, $P \cdot I \cdot A$, by a "reverse reaction". (Other reverse reactions, such as $P^+ \cdot I \rightarrow P \cdot I^+$ or $P^+ \cdot I \cdot A \cdot Q^- \rightarrow P^+ \cdot I \cdot A^- Q$ are possible, but less work has been done in these areas. Thus only the reverse ET from A^- to P^+ will be discussed here.) This reverse reaction has been extensively studied in bacteria [28,29,31,32, 176–178], and again it is found that the rate is activationless at low temperatures. This additional support for nuclear tunneling theories is interesting in itself, but there are several other important features which should be discussed.

First, it must be remembered that this reverse reaction does not normally occur (to an appreciable extent) in vivo. In fact, the sluggishness of this reaction is critical for the high efficiency of electron transport normally achieved by photosynthetic systems. If the reverse reaction were to occur readily, the light energy would simply be converted into heat energy (through phonon coupling) rather than into chemical energy through oxidation–reduction reactions (charge separation). However, in vitro studies of model systems have failed to reproduce the slow rates of the in vivo systems.

Several reasons for the slowness of this reaction in vivo have been suggested:
(a) Inverted behavior, since typically $-\Delta G_{rev} > \Delta G_{forward}$.
(b) H_{ab} changes, since the orbitals involved in the forward and reverse reactions are different. Also, orientation effects may be important.
(c) H_{ab} changes due to a lengthening of the separation distance between reactants which occurs after the forward reaction.
(d) Coupling to specific protein modes "tunes" the system for efficient energy level matching in the forward direction only, as suggested by Sarai [53,54].

These points may be evaluated in light of the available data. Point (a) alone does not seem to explain the failure of the model systems to reproduce the slow rates found in vivo. Evidently, reducing the complexity of the system changes either ΔG, E_r or H_{ab} for the reverse reaction. A change in protein conformation, for example, could conceivably explain the unexpectedly fast rates in model systems.

As for point (c), it is difficult to understand how the distance between reactants could change appreciably in a rigid medium in the time scale of these experiments. However, a change in H_{ab} could still occur by mechanism (b).

Finally, coupling to specific protein modes (d) is an interesting possibility. These modes are reasonably well-spaced and do not represent a continuum as in homogeneous solution. Thus, while isoenergetic donor–acceptor levels are available in the forward case, matching may not easily occur in the reverse direction. Unfortunately, the presently available information concerning the reverse ET is insufficient to unravel the details of its mechanism.

A second interesting aspect of the reverse reaction involves the rate behavior in the activated region. This reaction exhibits an apparent negative activation energy, the rate decreasing with increasing temperature (Fig. 8). Theoretically, as pointed out by several authors, this can occur if the product potential surface intersects the minimum of the reactant potential surface ($\Delta E = E_r$, Fig. 4). Such a reaction, although often referred to as "activationless", can exhibit a small negative activation barrier at elevated temperatures. However, activationless ET processes are normally quite fast, so the slowness of this reaction (in vivo, at least) points to the existence of a barrier and tends to discredit the above explanation.

Other explanations have been advanced:
(a) Variation of donor–acceptor distance with temperature.
(b) A competing reaction channel with different E_{act}.
(c) Coupling to protein soft modes.
(d) Frequency change during electron transfer, causing a temperature-dependent ΔG_{rxn} (as suggested by Kakitani and Kakitani [52]).

Again, it is not obvious that the distance can change significantly in rigid

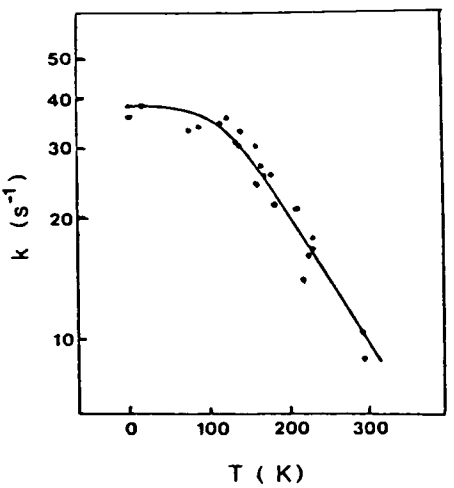

Fig. 11. Temperature dependence of the kinetics of the reverse reaction between P^+ and A^- in *Rps. sphaeroides*. This figure is adapted from ref. 16.

media, as suggested in (a). Further, one would expect such a change to affect the forward rate as well. This is not observed. A competing reaction channel may exist (b) but no evidence for this has been reported. Suggestion (c) implies that coupling to protein soft modes in the reverse reaction causes the efficiency of energy level matching to decrease as the temperature increases. Reaction from vibrationally excited states would be less favorable than from the ground (or low) vibrational states. Finally, explanation (d) points out the possibility of a change in entropy during electron transfer dominating the effect of temperature on rate. More work is needed to establish the cause of this unusual behavior with certainty.

In summary, there have been many attempts to explain the overall rate vs. temperature behavior of both the forward and reverse reactions of various biological systems. Most of the explanations attribute the break in the curve and the leveling off of the rate at low temperature to the onset of nuclear tunneling, as discussed in detail in the theoretical section. Nearly all of the discussion in the literature has focused on nuclear tunneling as the cause of such behavior. There is, however, evidence that other explanations need to be considered carefully before settling on nuclear tunneling as the only solution. Some of this evidence is presented below. Explanations of these rate vs. temperature curves which do not invoke tunneling will also be presented.

Hales [179] has suggested that the biological temperature dependences are caused by expansion or contraction of the components. He uses a coefficient of linear expansion for the proteins to fit the *C. vinosum* data (and the data for the back electron transfer from primary acceptor to donor in *R. rubrum*).

According to Hales, the "break" in the curves is due to discontinuity in α, which can occur when the binding of the medium suddenly changes at a given temperature. He supports this notion by presenting data from the literature in which the critical temperature T_c, is nearly always ~ 150 K.

Since the critical temperature for most proteins is so similar, it is difficult to understand why the values obtained by Hales for expansion coefficients are so different (differing in sign as well as in magnitude). In addition, while the *R. rubrum* data can be matched with a change in transfer distance from 28 Å (at 0 K) to 31 Å (at 300 K), the *C. vinosum* data requires distances of 36 Å (at 0 K) and 20 Å (at 300 K). This seems physically implausible.

Blumenfield et al. [180] have studied the reduction of adrenal ferredoxin as a function of temperature using ESR. The protein was reduced at 77 K, then, following a temperature jump, the ESR spectrum was monitored. The spectrum became constant after several minutes. Below about 140 K, in 95/5 H_2O–ethylene glycol, no changes were observed. At higher temperatures, large changes were seen in the ESR spectra, which leveled off above 210 K. In 50/50 water–ethylene glycol, the transition to high temperature behavior began at ~ 200 K rather than 140 K and was much sharper. This work tends to show that (1) at least some reorganization is totally "frozen out" at low temperature, and (2) the exact behavior of a system depends on solvent.

In a recent Mössbauer study on *R. rubrum*, Parak et al. [181] found that a new channel of motion which is attributed to fluctuations between conformational substates, began to contribute above 170 K. It is interesting that a similar dependence on temperature was observed for the efficiency of photoinduced electron transfer in this species.

Hiltner et al. [182] studied the dynamic mechanical relaxation of several polyamino acids as a function of temperature. They found three relaxation maxima and while two occurred at T values above room temperature, the third was at 105–135 K, possibly due to the freezing out of side-chain motions.

Very recent temperature studies of electron transfer between simple inorganic reagents in glycerol also yield temperature-dependent activation energies, although the "break" in the curve is not sharp [183]. The results suggest that the ET rate vs. temperature behavior is controlled, at least in part, by the changing dynamics of solvent reorganization rate. In other words, at low temperature, the solvent reorganization rate is slow on the time scale of the experiment. The ET process thus produces a pair of species in an unfavorable environment, and the effective ΔE for the reaction is not the equilibrium value, but is a function of time (see section on inversion). Whether a change in solvent (or protein) dynamics is responsible for the reported biological temperature dependences is open to question.

In short, a relatively large body of data, most of it from biological systems, exists concerning the temperature dependence of ET reactions. However, due to the complex nature of the systems, care must be taken in interpreting the data. Biphasic behavior was often observed and results varied not only with the particular species involved, but with the method of sample preparation as well. At present there is incomplete agreement on the origin of the observed temperature dependences.

L. ISOTOPE EFFECTS

The discrepancies among the theoretical treatments of nonadiabatic ET in part reflect the complexity of biological systems since key parameters (ΔE, R, etc.) are often essentially unknown. For this reason, studies of simple small molecules may clarify certain aspects of the ET description. Determination of kinetic isotope effect (KIE) ratios is one approach.

Isotopic substitution on small inorganic complexes can often be a simple matter (e.g. $Fe(H_2O)_6^{2+/3+}$ and $Fe(D_2O)_6^{2+/3+}$) and leads to changes in the zero-point energy and (metal–ligand) stretching frequencies of the molecules. Both the height of the classical nuclear barrier and the width of the nuclear tunneling barrier are changed (see Fig. 12). Thus, rate differences are expected. In an early paper, Ulstrup and Jortner [41] discussed this point and predicted an inverse isotope effect ($k_H/k_D < 1$) when $\Delta E < E_r$ and a normal isotope effect when $\Delta E > E_r$.

Indeed, an inverse isotope effect has been observed [184]. Zamaraev and coworkers report an isotope effect of 0.4 for the reaction of excited (S_1) naphthalene (vs. d_8-naphthalene) with CCl_4 in vitreous solution at 77 K. No effect of solvent deuteration was found [184].

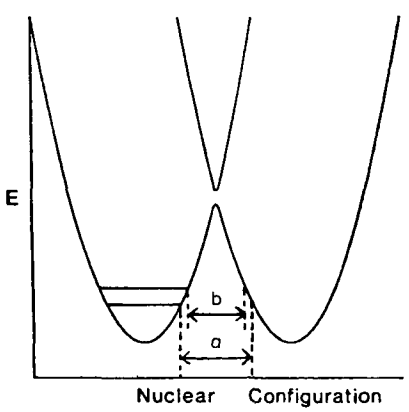

Fig. 12. The effect of isotopic substitution on the barrier width for nuclear tunneling. The heavier isotope corresponds to the thicker barrier a.

Other early work has involved the measurement of isotope fractionation ratios. DeChant and Hunt studied reactions of $(Cl)Cr(H_2O)(NH_3)_4^{2+}$ with both ^+H_3O and Cr(II). They obtained isotope effect ratios for $^{16}OH_2$ vs. $^{18}OH_2$ (ligand, rather than solvent substitution) of 1.017 for the *trans* complex and 1.007 for the *cis* complex. They suggested that a tetragonal distortion was occurring during the reaction [185,186]. Both ^{14}N vs. ^{15}N and ^{16}O vs. ^{18}O fractionation ratios in the reaction of Cr(II) with $Co(NH_3)_5(H_2O)^{3+}$ were studied by Murmann et al. [187].

Diebler et al. [188] investigated the reaction of various reductants with $(NH_3)_5Co(OH_2)^{3+}$ and $(NH_3)_5Co(OH)^{2+}$. They report isotope effects of 1.021 for the reaction of $Ru(NH_3)_6^{2+}$ with the aquo species, and 1.017 for its reaction with the hydroxo species. The behavior of V^{2+} and Eu^{2+} was similar to that of $Ru(NH_3)_6^{2+}$, while the ratio for the reaction of Cr(II) with $(NH_3)_5Co(OH)^{2+}$ was much larger, 1.046. Interestingly, when EDTA complexes of Fe^{2+}, Eu^{2+} and Cr^{2+} were used as reductants, these workers found fractionation ratios near unity [188]. Whether this is due to a decrease in the inner-sphere reorganization energy caused by the tetradentate ligand is unclear.

These early investigators all evaluated the data qualitatively as resulting from a change in bond length which occurs during electron transfer. Of course, great care must be taken in comparing rate ratios when the mechanism is unknown. In much of the early work, an inner-sphere mechanism is possible. We will concentrate here only on isotope effects in known outer-sphere type electron transfer reactions.

There are several studies of KIE in biological systems. Kihara and McCray [175] investigated both oxidation and reduction of cytochrome c in several photosynthetic bacteria. They report $\tau_{1/2}$ ratios of 1.25 to 1.56 for D_2O substitution of H_2O in whole cells and mitochondrial membrane fragments (the D_2O systems exhibit longer $\tau_{1/2}$ times). They suggest that electron transfer "takes place via the effective diffusional transfer of a hydrogen atom through a water bridge".

These workers also investigated the temperature dependence of the rates from 300 K to 77 K. They found an activationless region from 150 K to 77 K, and activated behavior ($E_a \sim 2.1$–2.3 kcal mol^{-1}) from 150 K to 300 K. The qualitative response of the system to temperature does not change upon substitution of D_2O for H_2O, but the $\tau_{1/2}$ values are increased by a factor of 1.3–1.4 throughout the entire temperature range [175]. Finally, the effects of using mixed solvents consisting of ethylene glycol, glycerol, and *p*-dioxane were studied, and it was concluded that there is no viscosity dependence of the rate.

In reporting their results, Kihara and McCray make special note of the fact that the measured isotope effects were $\sim 2^{1/2}$. Actually, the values

ranged from 1.25 to 1.56 and there may be no real significance to the exact factor $2^{1/2}$. This has also been pointed out by Ilan et al. [189] who studied cytochrome c oxidation and reduction, using both pulse radiolysis and temperature-jump methods. They found no KIE in the cyt c reduction by O_2^-, CO_2^- or $Fe(CN)_6^{4-}$. For cyt c oxidation, biphasic behavior was seen. Isotopic substitution of D_2O for H_2O did not affect the fast stage, but KIEs of 1.25 ± 0.2, depending on conditions, were found for the slow phase.

Later work by Kihara and McCray suggests that the reaction cannot be interpreted in terms of a simple bimolecular process [190]. Considering the possibility of a ferrocytochrome c/ferricyanide complex and analyzing the data in order to separate the ET rates from the effect of ferricyanide binding, they obtain $k_H/k_D = 1.37 \pm 0.07$.

Recent theoretical work from Jortner's group implies only a normal isotope effect should be found and makes several explicit predictions:
(a) The kinetic isotope effect (KIE) is a maximum at $\Delta E = 0$ and falls off with increasing ΔE until falling to a minimum ($k_H/k_D \sim 1$) when $\Delta E = E_r$.
(b) The value of the KIE increases when $\Delta E > E_r$.
(c) (k_H/k_D) is temperature-dependent, being larger at low temperature over some accessible temperature range. (k_H/k_D) is predicted to be proportional to $\exp(\alpha T^{-3})$. (However, more careful examination reveals that the magnitude of the prefactor will make this temperature dependence negligible.)

Buhks et al. [191] attempted to fit the data of Zwickel and Taube [192] to the $Cr(bipy)_2^{2+}$–$Co(NH_3)_6^{3+}$ reaction using the available data on Co $(NH_3)_6^{2+/3+}$ bond lengths. The predicted value of $k_H/k_D = 1.12$ lay well below the value of 1.36 found by Taube, and the participation of high-frequency "frozen" N–H modes was suggested. However, this reaction is not strictly second order, and is in fact quite complicated [193–195]. While it is still possible that the value reported by Taube corresponds to the second order portion of the reaction, further analysis is necessary.

Guarr et al. [196] have studied reactions of hexaaquo Fe(II) with various oxidants and have found reasonable agreement with the above predictions. In addition, these workers have investigated some of these reactions using $Fe(^{18}OH_2)_6^{2+}$ as the reductant. It is interesting to note that the k_{16}/k_{18} values obtained were generally less than the k_H/k_D ratios, which may indicate a small role for high frequency O–H "frozen" modes.

In 1975, Itzkowitz and Nordmeyer [197] found k_H/k_D ratios of 1.02 to 1.60 for reduction of pentaammine cobalt(III) by Cr(II) and U(II). These results have not yet been interpreted quantitatively in light of the recent theoretical developments.

Weaver and coworkers have investigated both the solvent isotope effect and ligand isotope effect on the formal potentials of a large number of transition metal redox couples in aqueous media [198–202]. They find that,

in many cases, the midpoint potential shifts several to several tens of millivolts upon solvent deuteration. This emphasizes the fact that a different type of contribution to k_H/k_D in electron transfer reactions can occur—a change in the effective driving force for the reaction. Thus, one must be extremely careful in interpreting results of isotopic substitution studies.

In a recent report, Weaver and Li [201] suggest that changes in O–H (or N–H) bond lengths are insufficient to account for the magnitude of the observed isotope-dependent reorganization energy which exists. Instead, they suggest that the stronger and more extensive hydrogen bonds formed in D_2O (vs. H_2O) could result in decreased rotational mobility of aquo ions. In other words, reorientation of solvent molecules around an aquo ion in D_2O requires more energy, since more hydrogen bonds are broken. A small change in this reorientation energy can lead to the observed large isotope effects.

In conclusion, although few reports of kinetic isotope effects in well-defined systems have appeared, it is clear that important information on the nature of the ET process can be provided. To this end, precise measurements on simple outer-sphere ET systems are needed.

M. SUMMARY

In summary then, although a vast amount of work has been done in the area of electron transfer, relatively few experiments have been designed to probe the quantum nature of the process. This is primarily because no appropriate theoretical framework was available to aid in the interpretation of the data.

Such a theory now exists. It is based on nonadiabatic multiphonon radiationless decay theory, and incorporation of such effects as frequency changes, bond length changes, and a dispersion of solvent modes is possible. Additional experimental data are needed to adequately test this theory.

Perhaps the greatest experimental effort has been in the area of the distance dependence of ET. However, many of the systems studied to date have been ill-defined with regard to important parameters such as ΔE and E_r. In addition, little is known concerning the effect of intervening material on the distance dependence. Differences in σ vs. π system, solvent vs. "frozen" solvent, or protein vs. homogeneous solution will surely be present. Both theoretical predictions and experimental tests of these differences are crucial to a complete understanding of the ET process.

Inversion is also an area creating a great deal of interest. Experiments in this field have been plagued by complications, and simple, well-defined systems are few. Reactions with rigid D–A separations hold more promise

than those in solution, and some reports of inversion with such systems have appeared.

The earliest reports concerning the quantum nature of ET involve the temperature dependence of ET rate in biological systems. In fact, theoreticians have relied quite heavily on fitting this early data in order to establish the validity of their expressions. But biological systems are by nature complex, and it is surprising that few temperature studies of simple systems have been reported. Such studies of nonadiabatic ET (using, for example, rigid matrices) would be of great value to both theorists and experimentalists. Further, it is important to clearly establish whether important parameters such as R, ΔE, or E_r can vary with temperature. If so, are these effects the real cause of the observed dependence of rate on temperature? Within the past two years, the activity on fixed distance ET in biological systems has increased dramatically, and this pace continues to accelerate. As such data become available, more detailed comparisons of theory and experiment, and of proteins and small molecules, will become viable.

Finally, an important area in which the quantum effects of ET can be investigated concerns the measurement of kinetic isotope effects (KIE). A systematic study involving substitution of several different atoms in a reactant would allow an estimate of the coupling parameters in the process. For example, the question of "frozen mode" involvement could be answered. Perhaps even more fundamental, KIE studies will help establish whether current ET theories are physically accurate.

REFERENCES

1 R.A. Marcus, J. Chem. Phys., 24 (1956) 966–978.
2 R.A. Marcus, Discuss. Faraday Soc., 29 (1960) 21–31.
3 R.A. Marcus, J. Chem. Phys., 43 (1965) 679–701.
4 R.A. Marcus, Ann. Rev. Phys. Chem., 15 (1964) 155–196.
5 N.S. Hush, J. Chem. Phys., 28 (1958) 962–972.
6 N.S. Hush, Trans. Faraday Soc., 57 (1961) 557–580.
7 J. Halpern, Q. Rev. Chem. Soc., 15 (1961) 207–236.
8 N. Sutin, Ann. Rev. Nucl. Sci., 12 (1962) 285–328.
9 N. Sutin, Acc. Chem. Res., 1 (1968) 225–231.
10 N. Sutin, Acc. Chem. Res., 15 (1982) 275–282.
11 D. DeVault, Q. Rev. Biophys., 13 (1980) 387–564.
12 R.D. Cannon, Electron Transfer Reactions, Butterworth, London, 1980.
13 D. DeVault and B. Chance, Biophys. J., 6 (1966) 825–847.
14 T. Kihara and B. Chance, Biochim. Biophys. Acta, 189 (1969) 116–124.
15 M.Y. Okamura, R.A. Isaacson, and G. Feher, Biochim. Biophys. Acta, 546 (1979) 394–417.
16 R.E. Blankenship and W.W. Parson in J. Barber (Ed.), Photosynthesis in Relation to Model Systems. Elsevier/North Holland, Amsterdam, 1979, pp. 71–114.

17 B. Chance, D. DeVault, H. Frauenfelder, R.A. Marcus, J.R. Schrieffer, and N. Sutin (Eds.), Tunneling in Biological Systems. Academic Press, New York, (1979).
18 V. Balzani, F. Bolletta, M.T. Gandolfi, and M. Maestri, Top. Curr. Chem., 75 (1978) 1–64.
19 K. Kalyanasundaram, J. Kiwi, and M. Grätzel, Helv. Chim. Acta, 61 (1978) 2720–2730.
20 K. Kalyanasundaram and M. Grätzel, Angew. Chem. Int. Ed. Engl., 18 (1979) 701–702.
21 J. Kiwi and M. Grätzel, J. Am. Chem. Soc., 101 (1979) 7214–7217.
22 M. Grätzel, Acc. Chem. Res., 14 (1981) 376–384.
23 J.-M. Lehn and J.-P. Sauvage, Nouv. J. Chim., 1 (1979) 449–451.
24 N. Sutin and C. Creutz, Adv. Chem. Ser., No. 168, (1978) 1–27.
25 N. Sutin, J. Photochem., 10 (1979) 19–40.
26 T. Meyer, Acc. Chem. Res., 11 (1978) 94–100.
27 P. LeLaive, J. Lee, H. Abruña, H. Sprintschnik, T. Meyer, and D. Whitten, Adv. Chem. Ser., No. 168 (1978) 28–43.
28 P. Avouris, K.S. Peters, and P.M. Rentzepis, Biophys. J., 21 (1978) 8a. Abstr M-Am-A1.
29 R.K. Clayton in B. Chance et al. (Eds.), Tunneling in Biological Systems. Academic Press, New York, 1979, pp. 377–386.
30 P.L. Dutton, T. Kihara, J.A. McCray, and J.P. Thornber, Biochim. Biophys. Acta, 226 (1971) 81–87.
31 E.S.P. Hsi and J.R. Bolton, Biochim. Biophys. Acta, 347 (1974) 126–133.
32 J.C. Romijn and J. Amesz, Biochim. Biophys. Acta, 423 (1976) 164–173.
33 K.J. Laidler, Can. J. Chem., 37 (1959) 138–147.
34 E. Sacher and K.J. Laidler, Trans. Faraday Soc., 59 (1963) 396–402.
35 B. Brocklehurst, Chem. Phys., 2 (1973) 6–18 and references therein.
36 V.G. Levich and R.R. Dogonadze, Dokl. Akad. Nauk. SSSR, 124 (1959) 123–126.
37 R.R. Dogonadze and Yu.A. Chizmadzhev, Dokl. Akad. Nauk. SSSR, 144 (1962) 1077–1080.
38 R.R. Dogonadze, A.M. Kuznetsov, M.G. Zakaraya, and J. Ulstrup, in B. Chance et al. (Eds.), Tunneling in Biological Systems. Academic Press, New York, 1979, pp. 145–171.
39 J.J. Hopfield, Proc. Natl. Acad. Sci. U.S.A., 71 (1974) 3640–3644.
40 J. Jortner, J. Chem. Phys., 64 (1976) 4860–4867.
41 J. Jortner and J. Ulstrup, J. Chem. Phys., 63 (1975) 4358–4368.
42 N.R. Kestner, J. Logan, and J. Jortner, J. Phys. Chem., 78 (1974) 2148–2165.
43 A.M. Kuznetsov, N.C. Søndergård, and J. Ulstrup, Chem. Phys., 29 (1978) 383–390.
44 S. Efrima and M. Bixon, Chem. Phys., 13 (1976) 447–460.
45 S.G. Christov, Ber. Bunsenges. Phys. Chem., 79 (1975) 357–371.
46 E. Buhks and J. Jortner, FEBS Lett., 109 (1980) 117–120.
47 B.S. Brunschwig, J. Logan, M.D. Newton, and N. Sutin, J. Am. Chem. Soc., 102 (1980) 5798–5809.
48 J. Jortner, J. Am. Chem. Soc., 102 (1980) 6676–6686.
49 E. Buhks and J. Jortner, J. Phys. Chem., 84 (1980) 3370–3371.
50 E. Buhks, M. Bixon, and J. Jortner, Chem. Phys., 55 (1981) 41–48.
51 P.O. Schmidt, J. Chem. Phys., 56 (1972) 2775–2787.
52 T. Kakitani and H. Kakitani, Biochim. Biophys. Acta, 635 (1981) 498–514.
53 A. Sarai, Chem. Phys. Lett., 63 (1979) 360–366.
54 S. Sarai, Biochim. Biophys. Acta, 589 (1980) 71–83.
55 L.N. Grigorov and D.S. Chernavskii, Biofizika, 17 (1972) 195–202.
56 P. Siders and R.A. Marcus, J. Am. Chem. Soc., 103 (1981) 741–747 and references therein.

57 G. Gamow, Z. Phys., 51 (1928) 204–212.
58 Note that even the very low (a few cm^{-1}) modes of λ_{out} can be involved in tunneling if the temperature is sufficiently low.
59 Simple Marcus theory provides for temperature independence in the special case of $\Delta E = E_r$.
60 T.F. Soules and C.B. Duke, Phys. Rev. B, 3 (1971) 262–274.
61 T. Förster, Naturwissenschaften, 33 (1946) 166–175.
62 D.L. Dexter, J. Chem. Phys., 21 (1953) 836–850.
63 K.F. Freed, Acc. Chem. Res., 11 (1978) 74–80.
64 M. Lax, J. Chem. Phys., 20 (1952) 1752–1760.
65 P.L. Dutton, Biochim. Biophys. Acta, 226 (1971) 63–80.
66 T. Kitagawa, Y. Ozaki, and Y. Kyogoku, Adv. Biophys., 11 (1978) 153–196.
67 R.E. Blankenship and W.W. Parson, Annu. Rev. Biochim., 47 (1978) 635–653.
68 R.A. Horne, J. Inorg. Nucl. Chem., 25 (1963) 1139–1146.
69 However, Horne [68] points out that this reaction probably occurs via an extended bridge mechanism.
70 M. Redi and J.J. Hopfield, J. Chem. Phys., 72 (1980) 6651–6660.
71 V. Balzani, F. Scandola, G. Orlandi, N. Sabbatini, and M.T. Indelli, J. Am. Chem. Soc., 103 (1981) 3370–3378.
72 J.F. Endicott and T. Ramasami, J. Am. Chem. Soc., 104 (1982) 5252–5254.
73 J.F. Endicott, T. Ramasami, D.C. Gaswick, R. Tamilasaran, M.J. Heeg, G.R. Brubaker, and S.J. Pyke, J. Am. Chem. Soc., 105 (1983) 5301–5310.
74 Several recent studies of reactions of zinc porphyrins in homogeneous solution have been reported, and distances of $R = 21$–22 Å (center-to-center) were found. This corresponds to edge-to-edge distances of 7–10 Å [75,76].
75 P.A. Carpelucci and D. Mauzerall, Ann. N.Y. Acad. Sci., 244 (1975) 214–237.
76 S.G. Ballard and D.C. Mauzerall, J. Chem. Phys., 72 (1980) 939–947.
77 J.V. Beitz and J.R. Miller, J. Chem. Phys., 71 (1979) 4579–4595.
78 J.R. Miller, J. Phys. Chem., 79 (1975) 1070–1078.
79 J.R. Miller, J. Phys. Chem., 82 (1978) 767–774.
80 J.R. Miller and J.V. Beitz, J. Chem. Phys., 74 (1981) 6746–6756.
81 K.I. Zamaraev, R.F. Khairutdinov, and J.R. Miller, Chem. Phys. Lett., 57 (1978) 311–315.
82 R.K. Huddleston and J.R. Miller, J. Phys. Chem., 86 (1982) 200–203.
83 J.R. Miller, J.A. Peeples, M.J. Schmitt, and G.L. Closs, J. Am. Chem. Soc., 104 (1982) 6488–6493 and references therein.
84 A. Kira, J. Phys. Chem., 85 (1981) 3047–3049.
85 A. Kira, Y. Nosaka, and M. Imamura, J. Phys. Chem., 84 (1980) 1882–1886.
86 R.F. Khairutdinov, N.A. Sadovskii, V.N. Parmon, M.G. Kuz'min, and K.I. Zamaraev, Dokl. Akad. Nauk. SSSR, 220 (1975) 888–891.
87 T. Guarr, M. McGuire, S. Strauch, and G. McLendon, J. Am. Chem. Soc., 105 (1983) 616–618.
88 S. Strauch, G. McLendon, M. McGuire, and T. Guarr, J. Phys. Chem., 87 (1983) 3579–3581.
89 B.H. Milosavljevic and J.K. Thomas, J. Phys. Chem., 87 (1983) 616–621.
90 F. Perrin, C.R. Acad. Sci. Paris, 178 (1924) 1978–1980.
91 M. Inokuti and F. Hirayama, J. Chem. Phys., 43 (1965) 1978–1989.
92 J.V. Alexandrov, R.F. Khairutdinov, and K.I. Zamaraev, Chem. Phys., 32 (1978) 123–141.
93 R.A. Marcus and P. Siders, J. Phys. Chem., 86 (1982) 622–630.

94 J.K. Thomas, Chem. Rev., 80 (1980) 283–299.
95 D. Meisel, M.S. Matheson, and J. Rabani, J. Am. Chem. Soc., 100 (1978) 117–122.
96 P.-A. Brugger, P.P. Infelta, A.M. Braun, and M. Grätzel, J. Am. Chem. Soc., 103 (1981) 320–326.
97 F.M. Martens and J.W. Verhoeven, J. Phys. Chem., 85 (1981) 1773–1777.
98 M.S. Tunuli and J.H. Fendler, J. Am. Chem. Soc., 103 (1981) 2507–2513.
99 L.Y.-C. Lee, J.K. Hurst, M. Politi, K. Kurihara, and J.H. Fendler, J. Am. Chem. Soc., 105 (1983) 370–373.
100 S. Hashimoto and J.K. Thomas, J. Am. Chem. Soc., 105 (1983) 5230–5237.
101 M.B. Robin and P. Day, Adv. Inorg. Chem. Radiochem., 10 (1967) 247–422.
102 N.S. Hush, Prog. Inorg. Chem., 8 (1967) 357–390.
103 N.S. Hush, Prog. Inorg. Chem., 8 (1967) 391–444.
104 H. Taube, Pure Appl. Chem., 44 (1975) 25–42.
105 J.E. Sutton and H. Taube, Inorg. Chem., 20 (1981) 3125–3134 and references therein.
106 J.E. Sutton and H. Taube, Inorg. Chem., 20 (1981) 4021–4023.
107 D.E. Richardson and H. Taube, J. Am. Chem. Soc., 105 (1983) 40–51 and references therein.
108 H. Taube in B. Chance et al. (Eds), Tunneling in Biological Systems. Academic Press, New York, (1979) pp. 173–197 and references therein.
109 K.A. Norton Jr. and J.K. Hurst, J. Am. Chem. Soc., 104 (1982) 5960–5966.
110 K.A. Norton, L.G. Hulett, D.J. Halko, and J.K. Hurst, in B. Chance et al. (Eds.), Tunneling in Biological Systems. Academic Press, New York, (1979) pp. 237–241.
111 M.J. Potasek and J.J. Hopfield, Proc. Natl. Acad. Sci. U.S.A., 74 (1977) 229–233.
112 M.J. Potasek and J.J. Hopfield, Proc. Natl. Acad. Sci. U.S.A., 74 (1977) 3817–3820.
113 Charge transfer bands have also been observed between the two partners of small ion pairs in solution, but as no distance information can be obtained in such systems, they will not be discussed further. The interested reader is referred to (for example): (a) J.C. Curtis, B.P. Sullivan, and T.J. Meyer, Inorg. Chem., 19 (1980) 3833–3839; (b) W. Rybak, A. Haim, T.L. Netzel, and N. Sutin, J. Phys. Chem., 85 (1981) 2856–2860; (c) J.C. Curtis and T.J. Meyer, Inorg. Chem., 21 (1982) 1562–1571.
114 R. Hoffman, A. Imamura, and W.J. Hehre, J. Am. Chem. Soc., 90 (1968) 1499–1509.
115 R. Hoffman, Acc. Chem. Res., 4 (1971) 1–9.
116 C.A. Stein and H. Taube, J. Am. Chem. Soc., 100 (1978) 1635–1637.
117 C.A. Stein and H. Taube, J. Am. Chem. Soc., 103 (1981) 693–695.
118 C.A. Stein, N.A. Lewis, and G. Seitz, J. Am. Chem. Soc., 104 (1982) 2596–2599.
119 C.A. Stein, N.A. Lewis, G. Seitz, and A.D. Baker, Inorg. Chem., 22 (1983) 1124–1128.
120 P. Pasman, F. Rob, and J.W. Verhoeven, J. Am. Chem. Soc., 104 (1982) 5127–5133.
121 H.M. McConnell, J. Chem. Phys., 35 (1961) 508–515.
122 D. Beratan and J.J. Hopfield, J. Am. Chem. Soc., 5. Am. Chem. Soc., 106 (1984) 1584–1984.
123 R.H. Austin and J.J. Hopfield, Electron Transp. Oxygen Util., [Int. Symp. Interact. Iron Proteins Oxygen Electron Transp.] (1980), C. Ho (Ed.), Elsevier, New York, 1982, pp. 73–80.
124 J.L. McGourty, N.V. Blough, and B.M. Hofman, J. Am. Chem. Soc., 105 (1983) 4470–4472.
125 S. Wherland and H.B. Gray, Proc. Natl. Acad. Sci. U.S.A., 73 (1976) 2950–2954.
126 A.G. Mauk, R.A. Scott, and H.B. Gray, J. Am. Chem. Soc., 102 (1980) 4360–4363.
127 a J.R. Winkler, D.G. Nocera, K.M. Yocom, E. Bordignon, and H.B. Gray, J. Am. Chem. Soc., 102 (1980) 4360–4363.
127 b K. Yocum, J.B. Shelton, W.A. Schroeder, G. Worosila, S.S. Isied, E. Bordignon, and H.B. Gray, Proc. Natl. Acad. Sci., U.S.A., 79 (1982) 7052–7055.

128 A.G. Mauk, E. Bordignon, and H.B. Gray, J. Am. Chem. Soc., 104 (1982) 7654–7657 and references therein.
129 a D.G. Nocera, J.R. Winkler, K.M. Yocom, E. Bordignon, and H.B. Gray, J. Am. Chem. Soc., 106 (1984) 5145–5150.
129 b S.S. Isied, C. Kuehn, and G. Worosila, J. Am. Chem. Soc., 106 (1984) 1722–1726.
130 J.L.Y. Kong and P.A. Loach, J. Heterocycl. Chem., 17 (1980) 737–744.
131 J.L.Y. Kong, K.G. Spears, and P.A. Loach, Photochem. Photobio., 35 (1982) 545–553.
132 J.S. Leigh Jr., D.F. Wilson, C.S. Owen, and T.E. King, Arch. Biochem. Biophys., 160 (1974) 476–486.
133 M.Y. Okamura, R.A. Isaacson, and G. Feher, Biochim. Biophys. Acta, 546 (1979) 394–417.
134 R.K. Gupta and T. Yonetani, Biochim. Biophys. Acta, 292 (1973) 502–508.
135 C.R. Bock, T.J. Meyer, and D.G. Whitten, J. Am. Chem. Soc., 97 (1975) 2909–2911.
136 R. Scheerer and M. Grätzel, J. Am. Chem. Soc., 99 (1977) 865–871.
137 J. Eriksen and C.S. Foote, J. Phys. Chem., 82 (1978) 2659–2662.
138 J.K. Nagle, W.J. Dressick, and T.J. Meyer, J. Am. Chem. Soc., 101 (1979) 3993–3995.
139 E. Vogelmann, S. Schreiner, W. Rauscher, and H. Kramer, Z. Phys. Chem. N.F., 101 (1976) 321–336.
140 L.V. Romashov, Yu.I. Kiryukhin, and Kh.S. Bagdasar'yan, Dokl. Phys. Chem. (Engl. Trans.), 230 (1976) 961–964.
141 U. Breymann, H. Dreeskamp, E. Koch, and M. Zander, Chem. Phys. Lett., 59 (1978) 68–70.
142 F. Scandola and V. Balzani, J. Am. Chem. Soc., 101 (1979) 6140–6142.
143 D.P. Rillema, J.K. Nagle, L.F. Barringer, Jr., and T.J. Meyer, J. Am. Chem. Soc., 103 (1981) 56–62.
144 F.M. Martens, J.W. Verhoeven, R.A. Gase, N.K. Pandit, and Th.J. de Boer, Tetrahedron, 34 (1978) 443–446.
145 D. Rehm and A. Weller, Israel J. Chem., 8 (1970) 259–271.
146 D. Rehm and A. Weller, Ber. Bunsenges. Phys. Chem., 73 (1969) 834–839.
147 R. Ballardini, G. Varani, M.T. Indelli, F. Scandola, and V. Balzani, J. Am. Chem. Soc., 100 (1978) 7219–7223.
148 M.T. Indelli and F. Scandola, J. Am. Chem. Soc., 100 (1978) 7733–7734.
149 W.L. Wallace and A.J. Bard, J. Phys. Chem., 83 (1979) 1350–1357 and references therein.
150 S.F. Fischer and R.P. Van Duyne, Chem. Phys., 26 (1977) 9–16.
151 S. Efrima and M. Bixon, Chem. Phys., 13 (1976) 447–460.
152 S. Efrima and M. Bixon, Chem. Phys. Lett., 25 (1974) 34–37.
153 C. Creutz and N. Sutin, J. Am. Chem. Soc., 99 (1977) 241–243.
154 C.D. Jonah, M.S. Matheson, and D. Meisel, J. Am. Chem. Soc., 100 (1978) 1449–1456.
155 C. Creutz, P. Kroger, T. Matsubara, T.L. Netzel, and N. Sutin, J. Am. Chem. Soc., 101 (1979) 5442–5444.
156 J.R. Miller, J.V. Beitz, and R.K. Huddleston, J. Am. Chem. Soc., 106 (1984) 5057–5068.
157 C.B. Duke and R.J. Meyer, Phys. Rev. B, 23 (1981) 2111–2125.
158 D.F. Calef and P.G. Wolynes, J. Phys. Chem., 87 (1983) 3387–3400.
159 R.P. Van Duyne and S.F. Fischer, Chem. Phys., 5 (1974) 183–197.
160 J.R. Miller, L. Calcaterra and G. Closs, J. Am. Chem. Soc., 106 (1984) 3047–3049.
161 A.J. Frank, M. Grätzel, A. Henglein, and E. Janata, Ber. Bunsenges. Phys. Chem., 80 (1976) 294–300.
162 A.J. Frank, M. Grätzel, A. Henglein, and E. Janata, Ber. Bunsenges. Phys. Chem., 80 (1976) 547–551.

163 K.J. Kaufmann, P.L. Dutton, T.L. Netzel, J.S. Leigh, and P.M. Rentzepis, Science, 188 (1975) 1301–1304.
164 K.J. Kaufmann, K.M. Petty, P.L. Dutton, and P.M. Rentzepis, Biochem. Biophys. Res. Commun., 70 (1976) 839–845.
165 M.G. Rockley, M.W. Windsor, R.J. Cogdell, and W.W. Parson, Proc. Natl. Acad. Sci. U.S.A., 72 (1975) 2251–2255.
166 W.W. Parson, Biochim. Biophys. Acta, 153 (1968) 248–259.
167 W.W. Parson, Biochim. Biophys. Acta, 189 (1969) 384–396.
168 R. Govindjee (Ed.), Bioenergetics of Photosynthesis. Academic Press, New York, (1975).
169 J. Barber (Ed.), Primary Processes of Photosynthesis. Elsevier/North Holland, Amsterdam, (1977).
170 B. Chance and M. Nishimura, Proc. Natl. Acad. Sci., U.S.A., 46 (1960) 19–24.
171 D. DeVault, J.H. Parkes, and B. Chance, Nature, 215 (1967) 642–644.
172 M. Siebert and D. DeVault, Biochim. Biophys. Acta, 205 (1970) 220–231.
173 W.W. Parson and G.D. Case, Biochim. Biophys. Acta, 205 (1970) 232–245.
174 M. Siebert and D. DeVault, Biochim. Biophys. Acta, 253 (1971) 396–411.
175 T. Kihara and J.A. McCray, Biochim. Biophys. Acta, 292 (1973) 297–309.
176 W.W. Parson, Biochim. Biophys. Acta, 131 (1967) 154–172.
177 P.A. Loach, M.C. Kung, and B.J. Hales, Ann. N.Y. Acad. Sci., 244 (1975) 297–319.
178 J.D. McElroy, D.C. Mauzerall, and G. Feher, Biochim. Biophys. Acta, 333 (1974) 261–277.
179 B.J. Hales, Biophys. J., 16 (1976) 471–480.
180 I.A. Blumenfeld, D.S. Burbaev, R.M. Davydou, L.N. Kubrina, A.F. Vanin, and R.O. Vilu, Biochim. Biophys. Acta, 379 (1975) 512–516.
181 F. Parak, E.N. Frolov, A.A. Kononenko, R.L. Mössbauer, V.I. Goldanskii, and A.B. Rubin, FEBS Lett., 117 (1980) 368–372.
182 A. Hiltner, J.M. Anderson, and E. Borkonski, Macromolecules, 5 (1972) 446–449.
183 M. McGuire and G. McLendon, to be published.
184 A.I. Fiskel, V.N. Parmon, and K.I. Zamaraev, Chem. Phys., 69 (1982) 135–139.
185 Sr. M.J. DeChant and J.B. Hunt, J. Am. Chem. Soc., 89 (1967) 5988–5989.
186 Sr. M.J. DeChant and J.B. Hunt, J. Am. Chem. Soc., 90 (1968) 3695–3699.
187 R.K. Murmann, H. Taube, and F.A. Posey, J. Am. Chem. Soc., 79 (1957) 262–265.
188 H. Diebler, P.H. Dodel, and H. Taube, Inorg. Chem., 5 (1966) 1688–1691.
189 Y. Ilan, R. Shinar, and G. Stein, Biochim. Biophys. Acta, 461 (1977) 15–24.
190 T. Kihara and J.A. McCray, Biochim. Biophys. Acta, 548 (1979) 417–426 and references therein.
191 E. Buhks, M. Bixon, and J. Jortner, J. Phys. Chem., 85 (1981) 3763–3766.
192 A.M. Zwickel and H. Taube, Discuss. Faraday Soc., 29 (1960) 42–48.
193 B.R. Baker and B.D. Mehta, Inorg. Chem., 4 (1965) 848–854.
194 Y. Narusawa, M. Kimura, and K. Nakano, Bull. Chem. Soc. Jpn., 47 (1974) 2017–2025.
195 T. Guarr and G. McLendon, unpublished results.
196 T. Guarr, E. Buhks, and G. McLendon, J. Am. Chem. Soc., 105 (1983) 3763–3767.
197 M.M. Itzkowitz and F.R. Nordmeyer, Inorg. Chem., 14 (1975) 2124–2129.
198 M.J. Weaver and S.M. Nettles, Inorg. Chem., 19 (1980) 1641–1646.
199 E.L. Yee, R.J. Cave, K.L. Guyer, P.D. Tyma, and M.J. Weaver, J. Am. Chem. Soc., 101 (1979) 1131–1137.
200 M.J. Weaver, P.D. Tyma, and S.M. Nettles, J. Electroanal. Chem. Interfacial Electrochem., 114 (1980) 53–72.
201 M.J. Weaver and T.T.-T. Li, J. Phys. Chem., 87 (1983) 1153–1157.
202 M.J. Weaver and E.L. Yee, Inorg. Chem., 19 (1980) 1936–1945.

203 T. Guarr, M. McGuire, and G. McLendon, J. Am. Chem. Soc., 107 (1985) 5104–5111.
204 V. Krongauz and J.R. Miller, to be published.
205 B.S. Brunschwig, S. Ehrenson, and N. Sutin, J. Am. Chem. Soc., 106 (1984) 6858–6859.
206 E. Buhks, R.G. Wilkins, S.S. Isied, and J.F. Endicott in D.B. Rorabacher and J.F. Endicott (Eds.), Mechanistic Aspects of Inorganic Reactions. ACS Symp. Ser., 198 (1982) 213–233.
207 a B. Anderes and D.K. Lavallee, Inorg. Chem., 22 (1983) 2665–2666.
207 b M.J.K. Geno and J.H. Dawson, Inorg. Chem., 23 (1984) 1182–1183.
208 T.T.-T. Li and M.J. Weaver, J. Am. Chem. Soc., 106 (1984) 6107–6108.
209 D. Möbius, Acc. Chem. Res., 14 (1981) 63–68.
210 a T.L. Netzel, M.A. Bergkamp, and C.K. Chang, J. Am. Chem. Soc., 104 (1982) 1952–1957.
210 b M.R. Wasielewski and M.P. Niemczyk, J. Am. Chem. Soc., 106 (1984) 5043–5045.
210 c T.A. Moore, D. Bust, P. Mathis, J.-C. Mialocq, C. Chachaty, R.V. Bensassoon, E.J. Land, D. Doizi, P.A. Liddell, W.R. Lehman, G.A. Nemeth, and A.L. Moore, Nature, 307 (1984) 630–632.
211 J.R. Miller, L.T. Calcaterra, and G.L. Closs, J. Am. Chem. Soc., 106 (1984) 3047–3049.
212 S.E. Peterson-Kennedy, J.L. McGourty, and B.M. Hoffman, J. Am. Chem. Soc., 106 (1984) 5010–5012.
213 G.L. McLendon, J.R. Winkler, D.G. Nocera, M.R. Mauk, A.G. Mauk, and H.B. Gray, J. Am. Chem. Soc., 107 (1985) 739–740.
214 K.P. Simolo, G.L. McLendon, M.R. Mauk, and A.G. Mauk, J. Am. Chem. Soc., 106 (1984) 5012–5013.
215 G. McLendon and J.R. Miller, J. Am. Chem. Soc., 107 (1985) in press.
216 a T.L. Poulos and A.G. Mauk, J. Biol. Chem., 255 (1983) 7369–7873.
216 b F.R. Salemme, J. Mol. Biol., 102 (1976) 563–568.
217 J.R. Miller and G. McLendon, J. Am. Chem. Soc., submitted for publication.
218 a K.F. Freed, Chem. Phys. Lett., 97 (1983) 489–493.
218 b A. Warshel and A.K. Churg, J. Mol. Biol., 168 (1983) 693–697.
219 R.A. Marcus and N. Sutin, Biochim. Biophys. Acta, in press: in this review, the authors suggest $\lambda \simeq 0.7$ V in protein–protein reactions.
220 [a]C. Franco and G. McLendon, Inorg. Chem., 23 (1984) 2370–2372; [c]Proc. NATO Workshop on Photocatalysis. Reidel Press (1986).
221 J. Allen, J. Colvin, D. Stimson, C. Flynn and H. Stapleton, Biophys. J., 38 (1982) 299.
222 [a]B.S. Brunschwig, C. Creutz, A.H. Macartney, T.-K. Sham and N. Sutin, Discuss. Faraday Soc., 74 (1982) 113–127, cf. [b]D.J. Szalda, D.H. Macartney and N. Sutin, Inorg. Chem., 23 (1984) 3473–3479.
223 D. Mauzerall and S. Ballard, Ann. Rev. Phys. Chem., 33 (1982) 377–427.
224 T. Ramasami and J.F. Endicott, J. Am. Chem. Soc., 107 (1985) 359–396.
225 R.M. Nielson and S. Wherland, J. Am. Chem. Soc., 107 (1985) 1505–1510.
226 M.J. Weaver and T. Gennett, Chem. Phys. Lett., 113 (1985) 213–218.
227 E.M. Kosower, J. Am. Chem. Soc., 107 (1985) 1114–1118.